# Observations Pertaining to the Origin and Ecology of Microorganisms Recovered From the Deep Subsurface of Taylorsville Basin, Virginia

T. C. ONSTOTT

Department of Geosciences
Princeton University
Princeton, New Jersey, USA

T. J. PHELPS

Environmental Sciences Division
Oak Ridge National Laboratory
Oak Ridge, Tennessee, USA

F. S. COLWELL

Idaho National Engineering and Environmental Laboratory
Idaho Falls, Idaho, USA

D. RINGELBERG
D. C. WHITE

Center for Environmental Biotechnology
University of Tennessee
Knoxville, Tennessee, USA

D. R. BOONE

Environmental Sciences and Engineering
Oregon Graduate Institute of Science and Technology
Portland, Oregon, USA

(continued)

Received 29 August 1997; accepted 30 March 1998.

This research was supported by grant 230377-A-F1 from the Environmental Science Research Center, Pacific Northwest National Laboratories through contract DE-AC06-76RLO 1830 and by grant DE-FG02-94ER61821 to T.C.O., through contract DE-AC07-76ID01570 to F.S.C., and by grant DE-FG02- 96ER62163 to D.C.W. and D.B., all from the Subsurface Science Program, managed by F. J. Wobber of the U.S. Department of Energy. We are extremely grateful to R. Vierbuchen and C. Dengo of EXXON Corporation for providing access to the petrophysical logs for the various exploration wells in the Taylorsville Basin. We are also indebted to B. Fulmer and his staff of the Division of Oil and Gas within the Virginia Department of Mines, Minerals, and Energy for releasing the mud log of the Wilkins 1.

Current address for D. Ringelberg is Waterways Experiment Station, CEWES-EP-P, 3909 Halls Ferry Dr., Vicksberg, Mississippi 39180-6199, USA.

D. C. White is also at the Environmental Sciences Division, Oak Ridge National Laboratory.

Address correspondence to Dr. T. C. Onstott, Department of Geosciences, Princeton University, Princeton, NJ 08544, USA.

Geomicrobiology, 15:353–385, 1998

0149-0451/98 $12.00 + .00

J. P. MCKINLEY
T. O. STEVENS
P. E. LONG

Battelle Pacific Northwest National Laboratories
Richland, Washington, USA

D. L. BALKWILL

Department of Biological Sciences
Florida State University
Tallahassee, Florida, USA

W. T. GRIFFIN

Golder Associates
Oak Ridge, Tennessee, USA

T. KIEFT

Department of Biology
New Mexico Institute of Mining and Technology
Socorro, New Mexico, USA

*To understand the conditions under which microorganisms exist in deep hydrocarbon reservoirs, sidewall cores were collected from a natural gas–bearing formation, 2800 m below the surface in Taylorsville Basin, Virginia. Data from chemical and microbial tracers and controls indicate that the interiors of some sidewall cores contained microorganisms indigenous to the rock formation. The cultured microorganisms were composed primarily of saline-tolerant, thermophilic fermenting, Fe(III)-reducing, and sulfate-reducing bacteria (1 to $10^4$ cells/g). The physiological capabilities of the cultured microorganisms are compatible with the temperature (76° C), pressure (32 MPa), and salinity (≈0.8 wt.% NaCl equivalent) in the sampled interval. The petrological data indicated that the strata contain intercrystalline pores of micrometer size, that occur between late diagenetic cement in siltstone and within cross-cutting, mineralized fractures in shale. These pores made up only 0.04% of the rock volume, were mostly gas-filled, and were interconnected by pore throats with diameters <0.04 μm. Because the pore throats are smaller than known bacteria, the cultured microorganisms were probably trapped within the larger pores containing alkaline, brackish, formation water. The total phospholipid fatty acid concentration of the rock samples yielded a cellular concentration equivalent to $4 \times 10^5$ cells/g, much greater than had been determined by enumeration of the cultured bacteria. This may have resulted from either inhibition of dephosphorolation reactions within pores filled with reduced gases, such as methane, or the inability to culture >0.1% of the viable bacteria. The recovery of living bacteria from such an austere environment represents one of the most remarkable examples of microbial survival yet reported.*

**Keywords** deep subsurface, hydrocarbon reservoirs, sulfate reduction, iron reduction, phospholipid fatty acid

Occurrences of living bacteria in oil field water have been reported for >70 years (Bastin 1926; Zobell 1947; Gurevich 1962; Rueter et al. 1994; L'Haridon et al. 1995). None of these

studies, however, determined whether the microorganisms recovered from the subsurface samples were indigenous to the deep, oil-bearing strata or had been introduced into the environment during the reservoir development. By adopting special coring techniques (Phelps et al. 1989), several investigators have reported evidence that some mesophilic bacterial communities are indigenous to aquifers and aquitards to a depth of at least 400 m (Balkwill and Ghiorse 1985; Balkwill 1988; Fredrickson et al. 1991). To ascertain the conditions under which indigenous thermophilic microbial communities might exist at the greater depths within gas- or oil-bearing reservoirs, similar coring methods were utilized to obtain deep, subsurface samples for microbial analyses from unexposed Triassic-age strata in the Taylorsville Basin, Virginia.

The rationale for selecting this basin rests on its geological, hydrological, and exploration history (Onstott et al. 1994). Unlike many of the Triassic, syn-rift basins of eastern North America, the Taylorsville Basin is almost entirely covered by a veneer of Cretaceous/Tertiary Coastal Plain sediments (Milici et al. 1991). As a result, the Triassic strata were not significantly penetrated by any drilling activity until 1986, at which time Texaco and Exxon initiated a limited series of gas exploration boreholes. Groundwater recharge is shunted through the highly permeable Coastal Plain cover sequence, hydrologically isolating the deep Triassic strata. This scarcity of boreholes and the hydrological isolation reduced the probability that bacteria from recent groundwater flow or drilling activity would be found in the low-permeability Triassic strata at great depth. In 1992, sidewall cores were collected from 2630 to 2795 m below land surface (mbls) at Thorn Hill 1, an exploratory well drilled near the center of Taylorsville Basin (T in Figure 1).

New species of saline-tolerant, thermophilic, metal-reducing, anaerobic bacteria were enriched in some of these core samples (Boone et al. 1995; Zhang et al. 1996; S.V. Liu et al. 1997; Y. Liu et al., unpublished). Although living bacteria have been reported in borehole water samples recovered from greater depths (3000 mbls, Stetter et al. 1993; 3500 mbls, Szewzyk et al. 1994), the bacteria from Thorn Hill 1 represent the deepest reported isolation from rock samples.

Chemical and microbial tracers (McKinley and Colwell 1996; Lehman et al. 1995) indicated that some of these samples were not significantly contaminated with surface materials or drilling fluids and suggested that the bacterial isolates were indigenous for the rock strata. In this study, we present additional microbial, petrological, geochemical, and petrophysical analyses of the sidewall cores and the results of borehole geophysical data that lend further support to the indigenous origin of these isolates. We conclude by comparing the microbial biomass and environmental setting of this site with those of other subsurface sites for which microbial communities have been identified.

## Methods and Procedures

### *Site Description*

The Triassic sediments of Taylorsville Basin form the Doswell Formation (Weems 1980) and are Early to Middle Carnian (230 Ma) in age (Cornet and Olsen 1990). At Thorn Hill 1, the Doswell Formation is ~2500 m thick. It is composed, from top to bottom, of the fluvial New Found Member, the paludal and lacustrine Falling Creek Member, the Stagg Creek sandstone, and the lacustrine Wilkins Member (Weems 1980; P.E. Olsen, pers. comm., 1995). At this location, the Doswell Formation is overlain by 680 m of Coastal Plain sediment, which ranges in age from Berriasian (136 Ma) to Miocene (5 Ma) (Robbins et al. 1975; Lowrie and Ogg 1986). One diabase intrusion was intersected during drilling at Thorn Hill 1 at a depth of 2129 mbls (Figure 2).

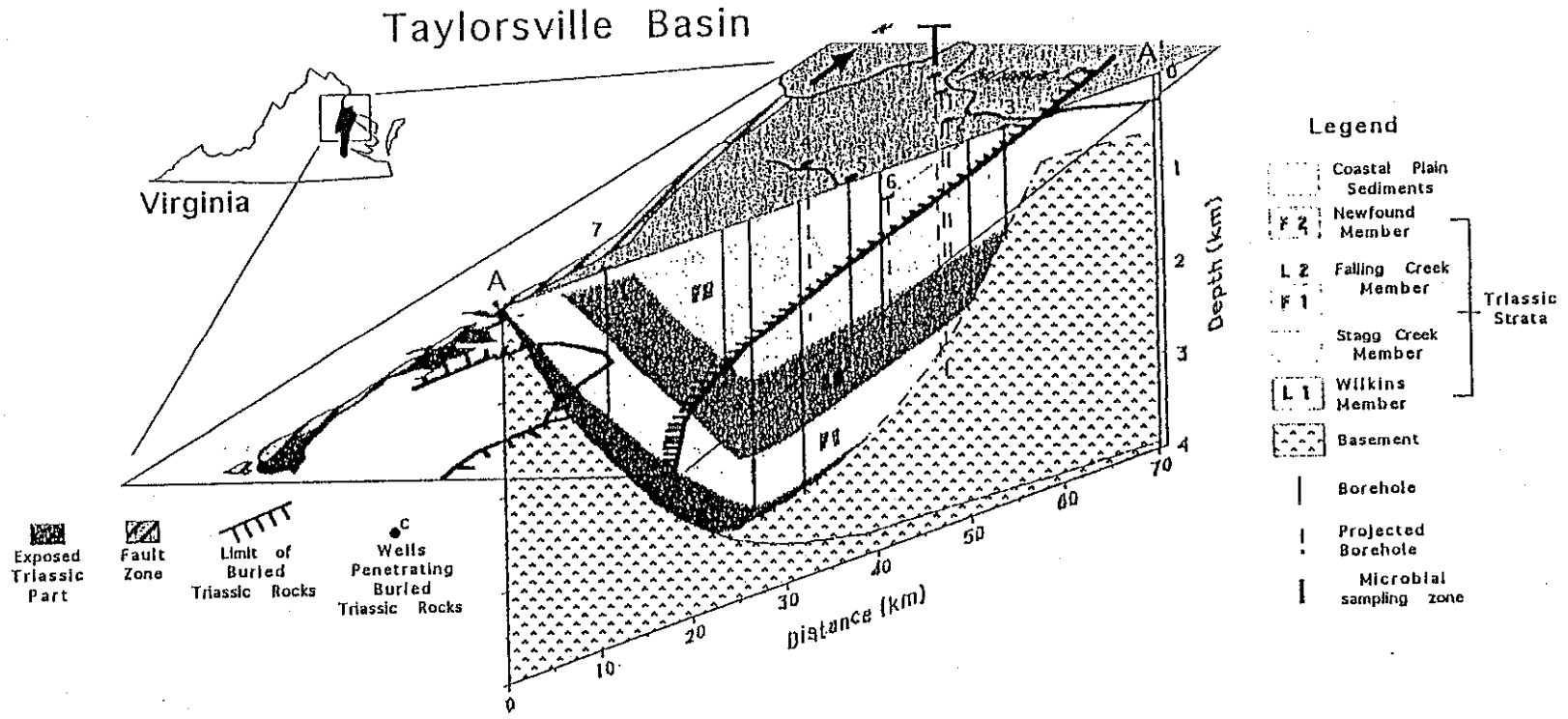


FIGURE 1 Characterization of the Taylorsville Basin. Upper left inset: location in northern Virginia. Oblique projection marks locations of cross-section for Figure 7. Locations of Thorn Hill 1 (T) and of the microbial sampling zone at Thorn Hill 1 are indicated and projected onto the cross-section A–A′. The cross-section records the approximate positions of the major stratigraphic units of the Triassic Doswell Formation. Also shown are positions of other exploration holes used to constrain basin structure and hydrostratigraphy (from Milici et al. 1991). Well numbers refer to those in Table 5.

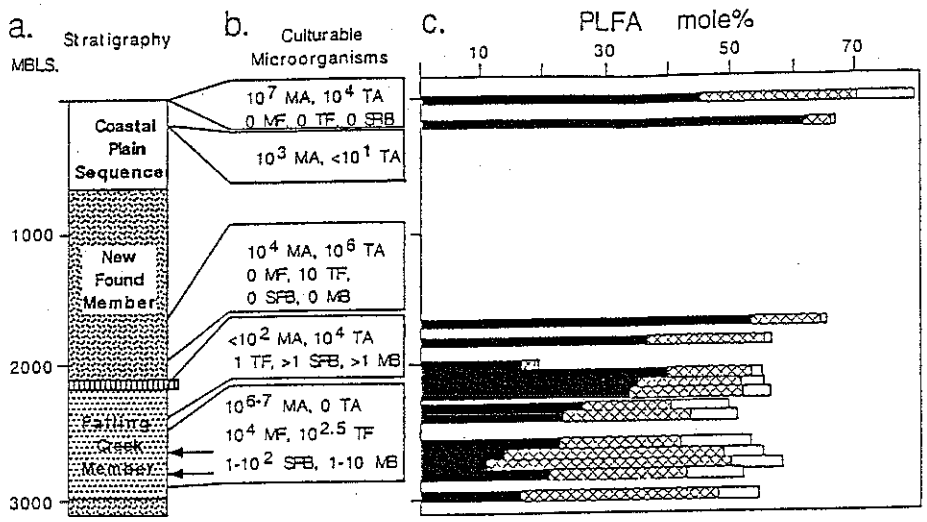


FIGURE 2 (a) Stratigraphic column for Thorn Hill 1, illustrating major lithological units. The vertical bars at 2200 mbls mark a diabase intrusive (thickness exaggerated for clarity). The bottom 120 m is Stagg Creek Member. Arrows demarcate the depth range of the sidewall coring. (b) Significant microbial components enriched from surface soil (top), make-up water from Coastal Plain Units (second from top), and drilling mud as a function of depth. MA = mesophilic aerobes (20°C); TA = thermophilic aerobes (60°C); MF = mesophilic anaerobic heterotrophs; TF = thermophilic anaerobic heterotrophs; SRB = thermophilic, heterotrophic, sulfate-reducing bacteria; MB = thermophilic methanogens. All media had 1.25–1.5 wt% NaCl. Numbers preceding these designations represent the cells/g (CFUs for aerobic enrichments and MPNs for anaerobic enrichments). (c) Variation of fatty acid composition of surface soil, a representative make-up water sample (one of four), and drilling mud samples as a function of depth. Cross-hatched pattern represents terminally branched saturated fatty acids. Open pattern represents mid-chain-branched saturates. Solid pattern represents monounsaturates.

### *Sample Collection*

Thorn Hill 1 borehole was initially drilled by Texaco in February 1992 to a depth of 770 m, penetrating the Coastal Plain sequence and the top of the Triassic strata (Figure 1). The Coastal Plain sequence was then geophysically logged and casing was set before drilling recommenced. Drilling continued until a depth of 3113 mbls was attained, in April 1992. During this phase of drilling, cuttings consisting of 5-mm rock chips were collected and washed for petrological analyses at 3- and 10-m intervals. Gas concentrations and compositions were logged every 3 m. Thirteen drilling mud samples and five cuttings samples were collected for microbial enrichments, community level physiological profiles (CLPP), phospholipid fatty acid (PLFA) analyses, and perfluoromethylcyclohexane tracer (PFT) analyses at selected horizons (Figure 2). Four make-up water samples from a well installed at ~130 mbls in the Middle Potomac sandstone (the Patapsco Formation in Maryland) as well as surface soil at the site were also sampled for CLPP and PLFA analyses and for microbial enrichments. These samples provided data on the microbial communities at the surface and shallow subsurface that could potentially contaminate the drilling fluid at greater depths. The drilling mud, cuttings, and make-up water were designated as DM, CU, and MW, respectively, followed by the depth in mbls.

Borehole geophysical logging was completed by Schlumberger (Houston, Texas) and ResTech Houston Inc. (Houston, Texas) within 24 h of termination of drilling mud circulation. A low-permeability zone in the Falling Creek Member of organic-rich shale, and siltstone interbedded with more porous sandstone and with high natural gas concentrations was selected for microbial sampling. The less-permeable horizons in this zone were targeted for sidewall coring to reduce the potential for drilling mud penetration and to increase the chances for recovery. The more-permeable sandstone layers were avoided for these reasons, even though the potential microbial biomass would have probably been greater in these layers. The sample zone was overlain by 500 m of Falling Creek Member and 1450 m of New Found Member and was underlain by 370 m of Falling Creek Member (Figure 2).

Two types of cores were collected at 20 depths between 2630 and 2799 mbls by using tools that were lowered down the borehole on a cable (Figure 3). Rotary sidewall cores were acquired with a small coring bit that was electronically locked into a position perpendicular to the axis of the borehole and then extended into the borehole wall by rotation. Five rotary sidewall cores (7.6 × 1.9 cm) were acquired from competent rock by drilling through the mud cake on the sides of the borehole. Percussion sidewall cores were acquired by using a tool that projected a small cylinder into the borehole wall with an explosive charge. Sixteen percussion cores (5.1 × 1.9 cm in diameter) were successfully recovered, but only from

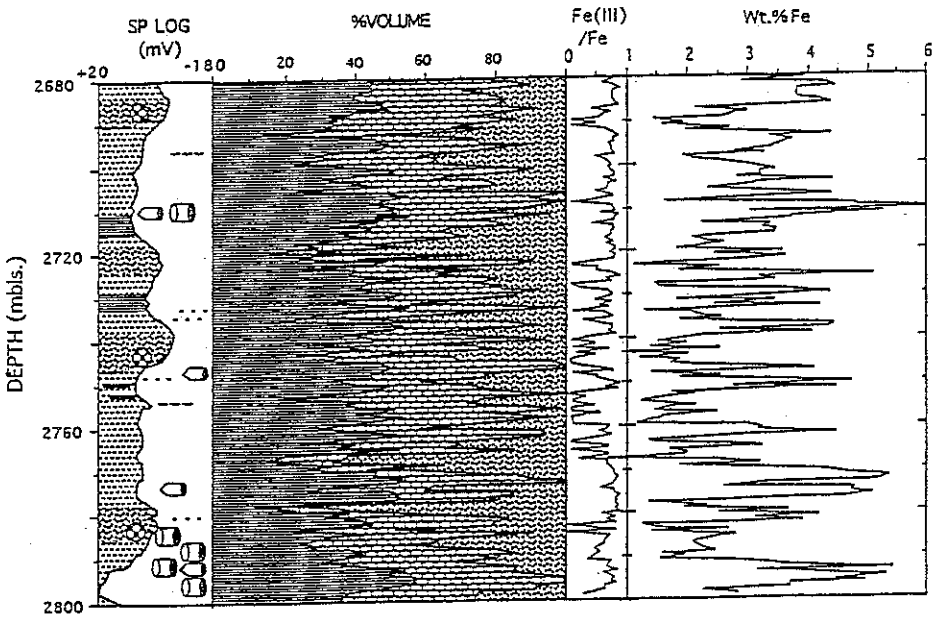


FIGURE 3 Variation in rock composition for the Falling Creek Member microbial sampling zone of Thorn Hill 1 as determined from analyses of petrophysical logs. From left to right: (1) SP log with reversed polarity to give the impression of an eroded lithology log. Patterns indicate presence of siltstone (speckled) vs shale (dash), pyrite (speckled circles), pyrobitumen (wavy line), and calcareous cement (brick). The 10 rotary (cylinders) and percussion (pointed cylinders) sidewall cores processed for microbiology are located between 2636 and 2801 mbls. Wavy dashed lines adjacent to SP profile delineate fractures detected by the petrophysical logs. (2) Modal percentages of clay + muscovite, carbonate, and albite + quartz. (3) Relative amount of ferric iron, plotted as Fe(III)/Fe. (4) Fe concentration in wt%.

he softer mud cake or less-indurated strata. The drilling mud was enriched in PFT prior to oring and was monitored during and after coring.

Of a total of 21 cores collected, 11 of the percussion cores were visibly compromised by drilling mudpack contamination and were archived. The remaining 10 cores were processed on-site in an anaerobic glove bag by paring off the outside surfaces with sterilized tools (Lehman et al. 1995). The rotary sidewall core parings, CS (or RP), and core interiors, RS, and the percussion core parings, PP, and core interiors, PC, were labeled by their depth below surface (Table 1). Two cores of Berea Sandstone baked at 600°C were processed under the same conditions as the sidewall cores to provide a procedural and sample-handling control. Fifteen processed sidewall core samples and the two control samples were shipped overnight on ice chests to various analytical laboratories for petrographic and geochemical analyses; for CLPP, PLFA, and PFT analyses; for direct counts by fluorescent tagging; and for microbial enrichments. Because of the low mass of the processed sidewall cores, not every sample could be subjected to the complete suite of analyses (Table 1). Percussion sidewall cores possessed much greater physical integrity than rotary sidewall cores, because the highly indurated rock formation fractured during the penetration of the percussion bit. Pared rotary sidewall cores, which represent the samples with the least potential microbial contamination, were successfully recovered from only three depths: 2793, 2794, and 2799 mbls (Table 1).

### *Microbial Enumeration, Biomass Estimates, and Tracer Assays*

The procedures for some of the microbial enrichments, the CLPP, the PLFA, and the PFT analyses of the Thorn Hill 1 samples (Table 1) have been presented elsewhere (Boone et al. 1995; Zhang et al. 1996; Lehman et al. 1995; and McKinley and Colwell 1996). As indicated in Table 1, CLPP analyses were performed on 2 percussion and 5 rotary sidewall core samples; PFT analyses were performed on 3 pared rotary sidewall cores and their parings; and PLFA analyses were performed on only 1 rotary sidewall core and its parings.

Enumeration of culturable bacteria was performed on select sidewall core samples (Table 1) and on the 13 drilling mud samples (Figure 2). Aerobic heterotrophs (AB) were enumerated by decimal dilution of drilling mud and sidewall core samples by shaking for 30 min in 0.1% Na-pyrophosphate at pH 7.0 followed by spread plate counts on 1% peptone, trypticase, yeast extract, glucose (PTYG) agar plates and on 0.01% trypticase, yeast extract, glucose, peptone (TYEGP) agar plates (Balkwill and Ghiorse 1985). These plates were incubated at 20, 30, and 60°C for up to 7 days before we counted the colonies that grew on each plate. Numbers of anaerobic bacteria were estimated by decimal dilution of sample in tubes of various enrichment media designed to promote growth of specific functional groups of anaerobic bacteria. The highest dilution in which growth occurred was assumed to approximate the inverse log of the population size, as determined by a most probable number (MPN) procedure (Stevens and McKinley 1995). All anaerobic samples were handled and inoculated in a controlled-atmosphere anaerobic chamber (5% $H_2$, 5% $CO_2$, 90% $N_2$). Enrichment media were degassed by boiling under a stream of $O_2$-free 80% $N_2$ and 20% $CO_2$ [for denitrifier bacteria (DNB) and dissimilatory iron-reducing bacteria (DIRB)] or prereduced [for dissimilatory sulfate-reducing bacteria (SRB) and methanogen bacteria (MB)] mineral salt solutions (Table 2 and Stevens et al. 1993) and were adjusted to a salinity of 1–1.5% NaCl and pH 7.4–8.0. Autotrophic enrichments contained 2 bar of $H_2$ in the head space as the sole electron donor. Heterotrophic enrichments contained a mixture of dilute carbon sources including 0.01% trypticase, yeast extract, glucose (TYEG) broth (Table 2). Anaerobic MPN tubes were incubated at 60°C for 6 months before enumeration.

Microscopic direct counts were performed on samples PC2637, RP2793, RS2799, and CS2799, which were fixed with formaldehyde in the field (Table 1). In the lab, the samples

TABLE 1 Summary of core sample analyses (grams of sample)

| Field no. | PC8647 | PC8648 | PC8909 | CS8910 | PC9032 | PC9121 | RS9161 | RP9161 | RS9164 | RP9164 | CS9164 | RS9180 | RP9180 | CS9180 | CS9188.5 |
|---|---|---|---|---|---|---|---|---|---|---|---|---|---|---|---|
| Sample no. | PC2636 | PC2637 | PC2716 | CS2717 | PC2754 | PC2781 | RS2793 | RP2793 | RS2794 | RP2794 | CS2794 | RS2799 | RP2799 | CS2799 | CS2801 |
| Thin-section | | | | 1.3 | | 2.6 | | | | | 3.8 | 2.2 | | 2.5 | 2.8 |
| Chemistry | 2.4 | | | 4.1 | 3.0 | | 4.0 | | 4.0 | | | 4.0 | | | |
| XRD | 0.3 | | 0.5 | 0.7 | 0.5 | 0.5 | 0.4 | | 0.4 | | | 0.5 | | | |
| Form | | 1.3 | | | | | | 0.4 | | | | 1.7 | | 5.3 | |
| PFT | | | | | | | 3.9[c] | 8.1[c] | 7.0[b] | | 3.0[b] | 9.8[a] | 5.6[a] | 3.2[a] | |
| CLPP | | | | | 0.4 | | | 0.5 | 0.5 | | | 0.5 | 0.5 | 0.5 | |
| PLFA | | | | | | | | | | | | 10.0 | 10.0 | 12.0 | |
| Culturable aerobes | | | 1.1 | | | | | 5.0 | | 10.0 | | 10.0 | 10.0 | 30.0 | |
| Culturable anaerobes | 0.2 | | | | 0.2 | 0.8 | 16.0 | 5.0 | 15.0 | 5.0 | 10.0 | 35.0 | 14.9 | 31.6 | |
| Total wt. | 2.9 | 1.3 | 1.6 | 6.1 | 4.1 | 3.9 | 24.3 | 19.0 | 26.9 | 15.0 | 16.8 | 73.7 | 41.0 | 85.1 | 2.8 |

PC = percussion core. RS = pared rotary side wall core. RP and CS = side and end parings of the rotary side wall core. Sample depth is given in feet below the surface and meters below the surface. Thin-section = samples prepared for petrographic and electron microprobe chemical analyses (T.C.O.). Chemistry = samples analyzed for whole-rock chemistry (J.P. McK.). XRD = samples analyzed by X-ray diffraction (J.P. McK.). Form = samples preserved in formaldehyde for direct counts (Nierzwicki-Bauer, R.P.I.). PFT = samples preserved in methanol for perfluorocarbon tracer analysis (J.P. McK.). CLPP = samples analyzed by community level physiological profile (Lehman et al. 1995). PLFA = samples analyzed by phospholipid fatty acid analyses (D.C.W.). Culturable aerobes = plate counts for aerobic, heterotrophic bacteria (D.L.B., T.K., and T.O.S.). Culturable anaerobes = MPN counts for anaerobic bacteria (D.R.B., T.O.S., and T.J.P.).

[a,b,c]Samples A, B, and C of McKinley and Colwell (1996), respectively.

TABLE 2 Results of perfluorocarbon tracers, microbial enumerations, and biomass estimates for sidewall core, control, and mud samples from Thorn Hill 1

| Analyses | DM2744 | PCs | RS2793 | RS2794 | RS2799 | Control |
|---|---|---|---|---|---|---|
| PFT | 790 | n.a. | 16 | 16 | 18–24 | 4–9 |
| AB (CFU)[a] | 6 | 5 | – | – | – | – |
| DNB (MPN)[a] | 0 | 2 | 1 | – | 0 | – |
| DIRB (Mix. Org.) (MPN)[a] | 5 | 3 | 4 | – | – | – |
| DIRB ($H_2/CO_2$) (MPN)[a] | 5 | 4 | 4 | 1 | 0 | – |
| SRB (Mix. Org.) (MPN)[a] | 2 | 2 | – | –0 | 0 | – |
| SRB ($H_2/CO_2$) (MPN)[a] | 2 | 1 | n.a. | – | 0 | – |
| M (Mix. Org.) (MPN)[a] | 2 | 3 | – | – | – | – |
| M ($H_2/CO_2$) (MPN)[a] | 2 | 4 | n.a. | – | 0 | – |
| PLFA | 188 | n.a. | n.a. | n.a. | 16 | 2.5 |
| CLPP | + | + | – | – | – | – |

[a]Log colony-forming units (CFUs) or MPN per gram. – = not detected. Detection limit ~0.3 cells/g. AB = aerobic bacteria. DNB = denitrifying bacteria. DIRB = dissimilatory iron-reducing bacteria. SRB = sulfate-reducing bacteria. M = methanogens. (Mix. Org.) = heterotrophic enrichments comprising four separate electron-donor groups (fermentation products, monomers, polymers, and aromatic hydrocarbons). ($H_2/CO_2$) = autotrophic enrichments where hydrogen is made the sole electron donor by pressurizing the headspace with an oxygen-free 50:50 mixture of $H_2$ and $CO_2$. All media contained a complement of minerals, salts, and trace metals (Stevens et al. 1993). SRB used a bicarbonate buffer with 20 mM PYR, lactate, FeSO4 and 2 mM $PO_4$. M used bacarbonate buffer, 50 mM acetate and MeOH, and 2 mM $PO_4$.

DM = drilling mud, PCs = composite result of percussion cores, RS = pared rotary sidewall cores, control = Berea sandstone cores baked at 600°C. PFT, perfluorocarbon tracer analyses in ng/g (McKinley and Colwell 1996). PLFA, phospholipid fatty acid in pmol/g; CS2799 yielded 10 pmol/g. CLPP, community level physiological profile: Biolog GN microplates were inoculated with extracts from drilling mud and core samples; each sample and a duplicate were incubated aerobically in the dark under humidification at 22°C for up to 1 week (Lehman et al. 1995); color development in the microplate was observed by absorbance at 590 nm using a microplate reader (+ = detected, – = not detected).

n.a. = not analyzed.

were powdered, stained with DNA-binding coumarin, and vortex-mixed, and the excess coumarin was removed by filtering with 0.2-$\mu$m polycarbonate filters. The filters were imaged by epifluorescence microscopy with a 100× oil-immersion lens.

### *Petrographic, Petrophysical, and Chemical Analyses*

Thin sections of six cores (Table 1) and 28 cuttings samples (from depths of 1725–3069 mbls) were prepared with blue dye epoxy and polished for analytical electron microscopy (EPMA). The elemental composition of various mineral phases was determined by EPMA. Eight coarse cutting samples from depths of 2326–3069 mbls were prepared for secondary electron microscopy (SEM). The modal abundance of minerals in the sidewall core of sandstone was determined by point-counting. Secondary mineral overgrowths were imaged by cathodoluminescence optical microscopy (Nuclide). The types of clay minerals were determined by X-ray diffraction (XRD) analyses of eight whole-rock samples (Table 1) and size separates for CS2799, the only sample with sufficient mass for this procedure.

Elemental analyses of six whole-rock samples were performed (Table 1). The sulfur concentration was determined by combusting the sample at 1350°C in the presence of oxygen to form $SO_2$. The $SO_2$ was then measured by an infrared detector. The phosphorous,

iron, and manganese concentrations were determined by fusing 0.2 g of sample with lithium tetraborate and lithium carbonate. The fusion product was then diluted to 100 mL with nitric acid and each element was quantified by inductively coupled plasma emission spectroscopy (ICP-AES). Samples were analyzed for total carbon by using a Leco CR-12 carbon analyzer (combustion) and for carbonate carbon by acidification and coulometric determination of the total $CO_2$ (ASTM, 1987). Total organic carbon was determined by the difference between total and carbonate carbon. The proportion of total Fe that is Fe(III) was determined for two samples of sufficient mass (RS2794 and RS2799) by measuring the amount of $V^{5+}$ produced from the oxidation of $V^{4+}$ by the reduction of Fe(III) to Fe(II). An empirical correction was made for the oxidation of $V^{4+}$ by the organic carbon present in the sample. The total Kjeldahl nitrogen content of the rock samples was determined by conversion to ammonium sulfate and colorimetric measurement of the ammonia concentration (Eaton et al. 1995).

The He porosity, air permeability, and Hg porosimetry were measured for RS2793 and RS2799, the only two samples with adequate sample size, by Core Petrophysics, Inc., Houston, Texas. The pore-size dimensions were derived from the Hg porosimetry data by using the method of Washburn (1921). Low-field magnetic susceptibility measurements were performed on a Bartington MS2 bridge.

### *Borehole Geophysical Modeling*

Utilizing the mineralogical, compositional, and petrophysical data available from the sidewall cores and cuttings, we forward-modeled the gamma spectrometry, photoelectric, gamma-density, neutron density, self-potential (SP), and resistivity logs.

The relative amounts of K- and Th-bearing minerals were determined by matching the wt% K and ppm Th given by the gamma spectroscopy log. These relationships are summarized by the following equations:

$$\text{wt\% K} = \sum(F_i \times K_i) \tag{1}$$

where wt% K is the gamma log estimate of K concentration, and $F_i$ is the volume fraction and $K_i$ the K concentration of each K-bearing mineral phase, respectively.

$$\text{ppm Th} = \sum(F_i \times \text{Th}_i) \tag{2}$$

where ppm Th is the gamma log estimate of Th concentration, and $F_i$ is the volume fraction and $\text{Th}_i$ the Th concentration of each Th-bearing mineral phase, respectively.

The sum of the volume fractions of each mineral phase has to equal 100% of the rock matrix:

$$1 = \sum F_i \tag{3}$$

The photoelectric log was modeled by the expression below, which is a volumetric average of photoelectric cross-sections for each mineral and fluid phase, weighted by the electron density:

$$\text{Pe}_{\text{bulk}} = \frac{\phi\{S_w \text{Pe}_w \rho e_w + [(1 - S_w)\text{Pe}_g \rho e_g]\} + (1 - \phi)\left[\sum F_i \text{Pe}_i \rho e_i\right]}{\phi\{S_w \rho e_w + [(1 - S_w)\rho e_g]\} + (1 - \phi)\left[\sum F_i \rho e_i\right]} \tag{4}$$

where $\phi$ is the porosity; $S_w$ is the water saturation or the fraction of water vs gas filling the pores; $Pe_w$, $Pe_g$, and $Pe_i$ are the photoelectric absorption cross-section indices for water, gas, and each mineral phase, respectively; and $\rho e_w$, $\rho e_g$, and $\rho e_i$ are the electron densities (effective densities measured by gamma log) for the water, gas, and each mineral phase, respectively.

A similar expression was used to model the neutron porosity logs:

$$N\phi_{bulk} = \phi\{S_w N\phi_w + [(1 - S_w)N\phi_g]\} + (1 - \phi)\left[\sum F_i N\phi_i\right] \tag{5}$$

where $N\phi_w$, $N\phi_g$, and $N\phi_i$ are the apparent neutron porosity for the water, gas, and each mineral phase, respectively. The porosity, $\phi$, was estimated by calculating the bulk density and comparing it with that given by the gamma density log, according to the following expression.

$$\rho_{bulk} = \phi\{S_w \rho e_w + [(1 - S_w)\rho e_g]\} + (1 - \phi)\left[\sum F_i \rho e_i\right] \tag{6}$$

The bulk density is the volumetric combination of the matrix density and fluid density. The matrix density was derived from the modal abundance and the electron densities of the mineral phases. The relative proportion of the liquid and gas components was determined by estimating the water saturation according to the following relationship from Alger et al. (1963).

$$\begin{aligned} S_w = (1 - F_c)^{-1}\{[0.81(R_w/R_f) + [F_c(R_c - R_w)/(2R_c)]^2]^{1/2} \\ -[F_c(R_c + R_w)/(2R_c)]\} \end{aligned} \tag{7}$$

where $F_c$ and $R_c$ are the volumetric fraction and resistivity of the clay component of the formation, $R_w$ is the resistivity of the formation water, and $R_f$ is the measured bulk formation resistivity. The resistivity of the formation water was determined from the SP log by using the following expression,

$$R_w = 0.85 R_{mf} 10^{1.3(SP+22)/(65+0.24T)} \tag{8}$$

where the SP is that of the strata with the lowest clay content, $T$ is the formation temperature (76°C), and $R_{mf}$ is the resistivity of the mud filtrate at formation temperature (1.13 ohm m). The formation water salinity in wt% NaCl equivalents was determined from the $R_w$, based on the results of Gondouin et al. (1957).

The permeability of the strata was estimated by using the expression of Coates and Dumanoir (1974):

$$K^{1/2} = C\left(0.077 + 1.55\rho_g - 0.627{\rho_g}^2\right)\phi^{2L}/(L^4 R_w/R_f) \tag{9}$$

where $K$ is the permeability in milliDarcy (mD), C is a calibration constant, and $L = \{3.75 - \phi + 1/2[\log(R_w/R_f) + 2.2]^2\}^{1/2}$.

The bulk gas volume was calculated from the porosity and saturation as follows:

$$V = \phi(1 - S_w)/\rho_m \tag{10}$$

where $V$ is the gas volume in mL/g and $\rho_m$ is the matrix density (g/mL). The concentration of hydrocarbons, primarily $CH_4$, in the gas was calculated from comparison of the gas log $CH_4$ with V.

Temperature logs and SP logs from the other exploration wells within the Taylorsville Basin were used to model the geothermal gradients and salinity gradients across the basin. The borehole temperatures were corrected for local perturbation of the formation temperature by the circulating drilling mud by using the approach of Lachenbruch and Brewer (1959). Formation fluid pressures were estimated from the weights of mud used in the exploration boreholes.

## Results

### *Microbiological Results*

#### *Drilling Mud Samples*

PLFA and CLPP analyses of the drilling mud samples indicated that the mud microbial communities were composed of a bimodal population of gram-negative aerobic heterotrophs and obligate anaerobes (Lehman et al. 1995). The relative abundance of culturable bacteria in the drilling mud samples (Figure 2b) indicated that the composition of the community shifted as a function of depth. The upper 2000 m were dominated by mesophilic aerobes ($10^6$–$10^7$ cells/g) and thermophilic aerobes ($10^4$–$10^6$ cells/g). Lipid analysis (MIDI, Inc., Newark, DE) of aerobic isolates from the drilling mud samples indicated that they were primarily *Pseudomonas stutzeri*. At 1700 mbls, thermophilic anaerobic heterotrophs began to appear in cultures derived from the drilling mud (Figure 2b) (10 cells/g). Beginning at 2000 and 2200 mbls and continuing to the bottom hole depth, the drilling mud samples yielded saline-tolerant, thermophilic, SRB (1–10 cells/g), MB (1–10 cells/g) (Figure 2b), and DIRB ($10^5$ cells/g). Mesophilic aerobes continued to dominate the drilling mud in this depth range, but thermophilic aerobes were not found below 2200 mbls.

At 2000 and 2200 mbls, the combined fraction of terminally branched saturates, predominantly in the iso-configuration, and mid-chain-branched saturates also increased (Figure 2c), suggesting that the proportion of obligate anaerobes (i.e., SRB) increased, whereas the aerobic community diminished (Lehman et al. 1995). CFU and MPN analyses of the drilling mud samples, however, indicated that the culturable aerobes still outnumbered the culturable anaerobes in the enrichments from the deepest drilling mud samples by at least 10 to 1 (Table 2).

#### *Sidewall Core Samples*

PFT concentration in the drilling mud was 40 times that measured in the rotary sidewall cores and 130 times that detected in the control sample. PLFA analyses indicates that the bacterial biomass in the drilling mud was 20 times that determined for the rotary sidewall core, RS2799 (Table 2). The PLFA concentration in the sidewall cores was 7 times that of the control sample. The culture results indicate that most of the bacterial biomass in the drilling mud and the percussion cores was aerobic heterotrophs. No aerobic bacteria were cultured from the rotary sidewall cores or from the control samples. Similarly, the CLPP analyses revealed the presence of mesophilic aerobic bacteria in the drilling mud and percussion sidewall core samples but failed to detect mesophilic aerobes in the rotary sidewall core samples (Table 2). The anaerobic enrichment cultures yielded DNB, DIRB, and SRB in the drilling mud, percussion sidewall cores, and rotary sidewall cores at $10^1$–$10^5$ cells/g, but none were enriched from the control samples (Table 2). Finally, MB were detected only in the drilling mud and the percussion sidewall core enrichments, but not in the rotary sidewall core enrichments and the control samples (Table 2).

Direct counts revealed intact cells in the rotary sidewall cores, but statistically justifiable estimates of the cells per gram could not be made, given the low sample mass available and the limited number of fields counted. The detection limit was $\sim 10^5$ cells/g.

### *Chemical and Mineralogical Composition*

The percussion sidewall cores were typically a mixture of rock fragments, drilling mud, and bit fragments. The rotary sidewall cores, on the other hand, were composed entirely of medium-gray, slightly calcareous siltstone; grayish-black, platy, organic-rich shale; and dark-gray argillaceous carbonate. The cores were finely laminated and some contained mineralized, cross-cutting veins.

The principal mineral phases were quartz, albite, illite, chlorite, ferroan calcite, ankerite, and muscovite, with minor biotite and sulfide. The albite was primarily the diagenetic alteration product of detrital K-feldspar and plagioclase, both of which had been almost completely replaced. The quartz frequently exhibited quartz overgrowths. The muscovite and biotite were typically deformed by compression from the surrounding albite and quartz grains in the siltstone, indicating a detrital origin. The biotite was partially replaced by a mixture of chlorite and pyrite. These observations indicate that the highly consolidated nature of the rock samples was attributable to a combination of dissolution and precipitation reactions and compression during the burial and a reductive diagenesis of these sediments.

The organic carbon concentrations of the rotary sidewall core samples were low, ranging from 0.2 to 1.3 wt% C (Table 3). This amount of carbon is readily accounted for by the minor detrital kerogen and secondary pyrobitumen observed in thin-section. The pyrobitumen in the veins recorded at least one episode of hydrocarbon migration during their burial history (Tseng 1997). The organic N concentrations (KjN in Table 3) indicate that the organic matter averages ~10 wt% N. The phosphorus concentrations range from 0.02 to 0.17 wt% P and appear to correlate with the organic carbon content (Table 3).

The carbonate concentration ranged from 0.5 to 2.5 wt% C (Table 3). This carbonate occurred primarily as a ferroan calcite and ankerite in pore-filling and vein-filling cements, although one sidewall core sampled a primary carbonate bed and another sidewall core intersected a 200-$\mu$m diameter carbonate concentration. Cathodoluminescence revealed multiple layers of carbonate in the veins, indicating many precipitation episodes by groundwater of various redox states.

The S concentrations of 0.01–0.11 wt% S (Table 3) indicate that the sulfide volumetric abundance never exceeded 0.04 vol%. This sulfur was entirely accounted for by pyrite, most of which exhibited a framboidal morphology and lined the pores of the siltstone and argillaceous carbonate. Euhedral pyrite also occurred in the shale. Pyrite, chalcopyrite, and sphalerite were present in the veins cutting across the shale layers of RS2799. These additional minerals contributed to the higher S content of that sample (Table 3).

The Fe contents of the shale (RS2799 and CS8910 in Table 2) were extremely high, ranging between 5 and 6.3 wt% Fe, whereas that of the siltstone samples (RS2793 and RS2794) were as low as 1.3 wt%. The measured Fe(III)/Fe ratios for RS2794 and RS2799 (Table 3) were 0.61 and 0.64, respectively. The oxidation state of the Fe did not change significantly between the two rock types, despite the large differences in the Fe content. Magnetic susceptibility ranged from $1.5 \times 10^{-8}$ to $3 \times 10^{-8}$ $m^3/kg$. These values are slightly less than the theoretical estimates, derived by assuming all of the measured Fe was paramagnetic (Collinson 1983) and indicate that <0.01 wt% magnetite is present. EPMA confirmed that Fe is concentrated in the clay fractions of these strata, residing in illite and chlorite. The Fe in illite in these types of sedimentary deposits is predominantly Fe(III) (Weaver and Pollard 1973), which could explain the observed values of Fe(III)/Fe.

TABLE 3 Chemical and petrophysical analyses of select sidewall core samples from Thorn Hill 1[a]

| | PC2636 | CS2717 | PC2754 | RS2793 | RS2794 | RS2799 |
|---|---|---|---|---|---|---|
| Elements[b] | | | | | | |
| Carb.-C | 0.57 | 0.95 | 2.39 | 0.53 | 2.39 | 1.52 |
| Org.-C | 0.92 | 1.30 | 2.82 | 0.49 | 0.21 | 0.80 |
| KjN | 0.11 | 0.12 | 0.13 | 0.07 | 0.01 | 0.05 |
| P | 0.09 | 0.08 | 0.17 | 0.02 | 0.07 | 0.06 |
| S | 0.01 | 0.02 | 0.01 | 0.01 | 0.01 | 0.11 |
| Fe | 6.47 | 6.26 | 6.55 | 1.26 | 3.98 | 5.17 |
| Fe(III)/Fe | n.a. | n.a. | n.a. | n.a. | 0.64 | 0.61 |
| Mn | 0.09 | 0.07 | 0.13 | 0.09 | 0.09 | 0.09 |
| Porosity[c] | n.a. | n.a. | n.a. | n.a. | 0.41 | 1.00 |
| Permeability[d] | n.a. | n.a. | n.a. | n.a. | 0.005 | 0.009 |
| Density[e] | n.a. | n.a. | n.a. | n.a. | 2.685 | 2.864 |

[a]PC2636 was collected from a 3-m-thick shale layer at the base of a 20-m-thick coarsening-upward sequence. The caliper log notes significant borehole washout at the depth of PC2636, indicating that the percussion core may be mostly mud pack. Because of the large caliper variation, the geophysical borehole logs for this depth interval were not modeled.

CS2717 was cored from a 4-m-thick shale layer at the top of a 14-m-thick fining-upward sequence. The resistivity values (ohm m) of the deeply penetrating and the intermediate-depth resistivity logs agree with each other and are significantly lower than the resistivity of the shallow resistivity log. This indicates that the drilling mud filtrate did not penetrate the rock formation.

PC2754 was taken from a 6-m-thick shale-carbonate layer. The high porosity and dip meter log indicate that this core penetrated a fractured zone. The resistivity values of the deeply penetrating and the shallow resistivity logs agree with each other and are significantly higher than the resistivity of the intermediate-depth resistivity log. This indicates that the drilling mud filtrate partially penetrated the rock formation.

RS2793, RS2794, and RS2799 were drilled from a 15-m-thick coarsening-upward sequence. From 2786 to 2796 mbls, the resistivity values of the deeply penetrating and the shallow resistivity logs agree with each other and are significantly higher than the resistivity of the intermediate-depth resistivity log. This indicates that the drilling mud filtrate partially penetrated the rock formation at this interval. From 2796 to 2801 mbls, the resistivity values (ohm m) of the deeply penetrating and the intermediate-depth resistivity logs agree with each other and are significantly lower than the resistivity of the shallow resistivity log. This indicates that the drilling mud filtrate did not penetrate the rock formation at this interval.

[b]All concentrations are in wt% of the elements.

[c]Porosity in % measured with He.

[d]Permeability in milliDarcy measured with an air permeameter probe.

[e]Density in g/mL.

n.a. = not analyzed.

The Mn concentrations ranged from 0.07 to 0.13 wt%. EPMA analyses of the carbonates indicated that these low levels of Mn can be entirely accounted for by the Mn(II) in the ferroan calcite cement.

### *Physical Properties*

The Hg and He porosity values for the samples RS2794 and RS2799 varied from 0.4% to 1.5% (Table 3). The Hg porosimetry data revealed that the pore throat radii ranged from 0.002 to 0.02 $\mu$m for samples RS2794 and RS2799 (Figure 4a) and that no more than 0.03% porosity could be present as interconnected micrometer-size pores. Image analyses of

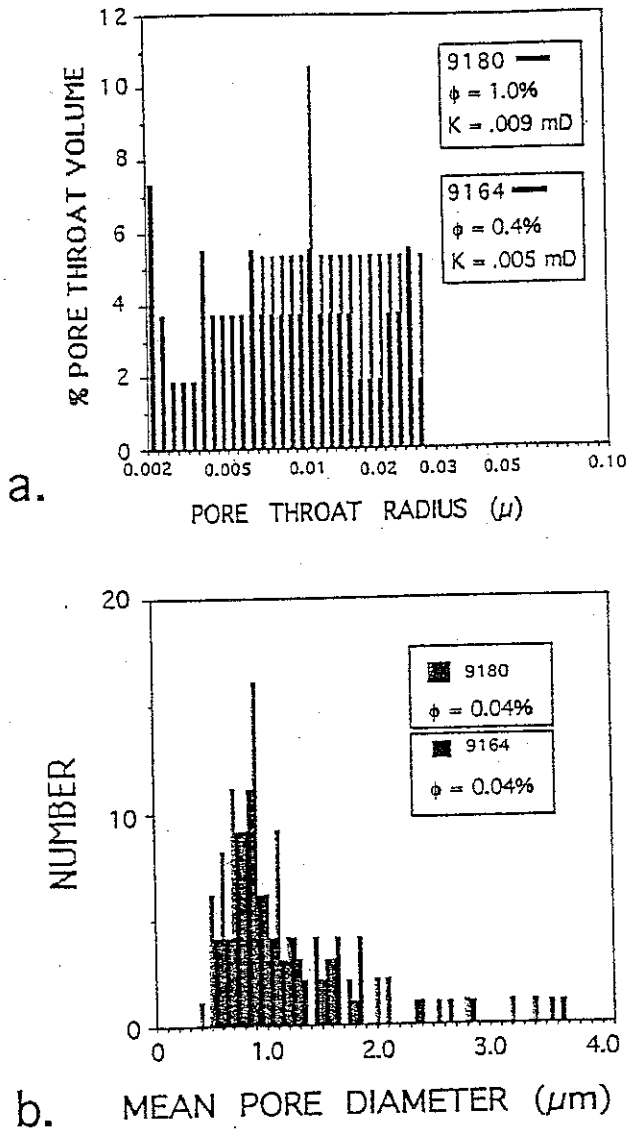


FIGURE 4 (a) Pore throat distribution for samples RS2794 and RS2799 determined by Hg injection according to the procedure of Washburn (1921). $\phi$ is the He porosity and $K$ is the gas permeability. (b) Pore diameter distribution determined by optical image analysis for samples RS2794 and RS2799. $\phi$ is the calculated porosity.

RS2794 and RS2799 did detect open pores with average diameters ranging from ~0.5 $\mu$m, the limit of optical measurement, to several micrometers (Figure 4b; Figure 5a) with a mean of slightly $<1$ $\mu$m. The volume fraction of observable pores for both samples was ~0.04%, which is consistent with the constraints imposed by the Hg porosimetry data.

The air permeability values for samples RS2794 and RS2799 were 5 and 9 $\mu$D, respectively. The permeability values reconstructed from the Hg porosimetry data by the approach of Swanson (1981) were $<1$ $\mu$D.

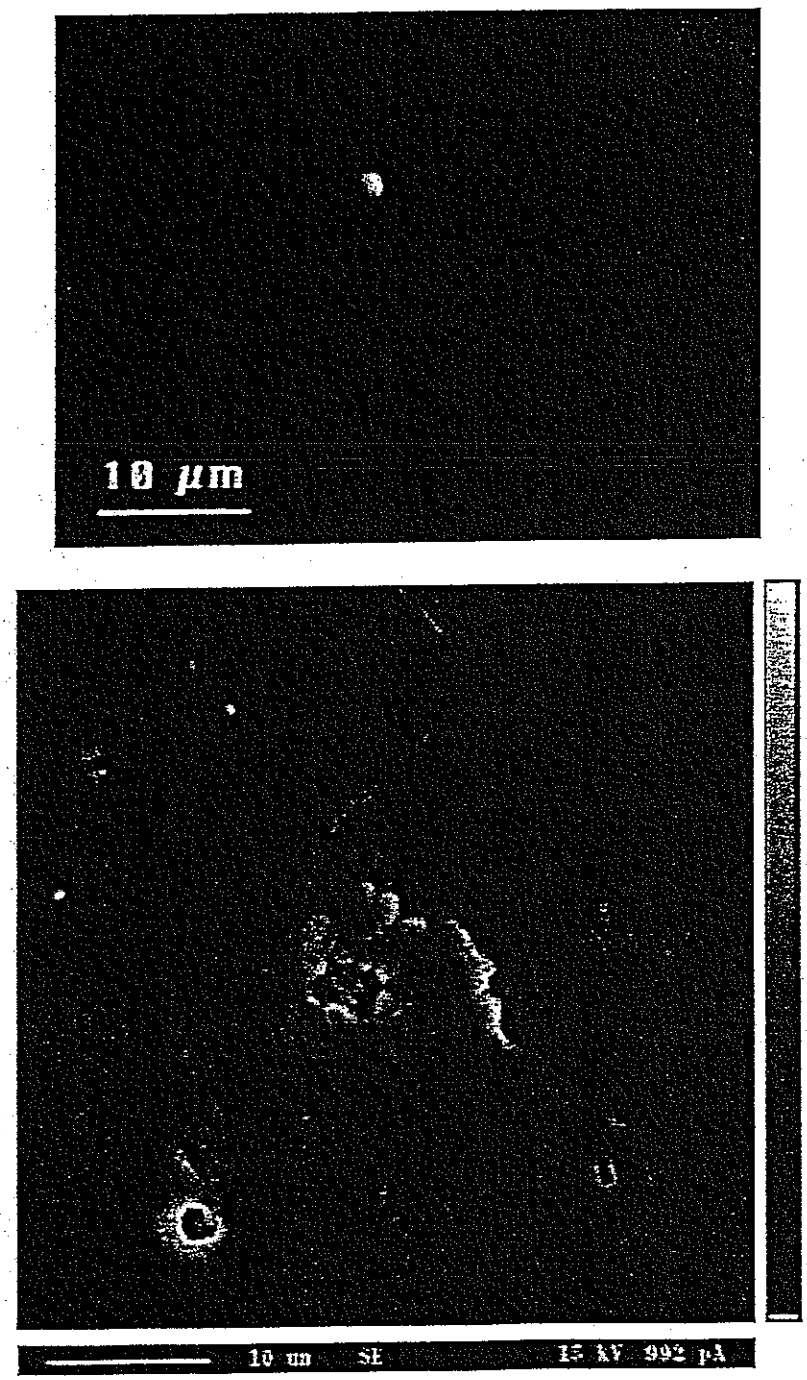


FIGURE 5 (Top) Epifluorescent photomicrograph of RS2794. Blue dye epoxy fluoresces in blue when excited by UV, revealing intergranular pores. (Bottom) SEM photomicrograph of a polished thin section of RS2794. Pore in center is lined with pyrite and clay. Smooth surfaces are quartz, and hummocky surfaces represent albitized K-feldspar. Intergranular interstices are seen as small (submicrometer) trenches that are discontinuous in the plane of the thin section.

Petrographic analyses indicated that the low porosity and permeability values are primarily caused by ductile deformation of clay and mica during burial compaction and by porosity reduction from carbonate and quartz cementation. Sample RS2799 contained more clay than sample RS2794 did, but the latter contained abundant pore-filling calcite cement (28% by volume). SEM analyses of sample RS2799 revealed secondary porosity that had developed by dissolution of detrital feldspars and quartz along their grain margins. SEM analyses of sample RS2794 indicated that the small voids existed at the interstices of the pore-filling calcite cement, framboidal pyrite (0.2–2 $\mu$m diameter) and clay (Figure 5). These occurrences coincide with the open pores that were optically identified thin section. Sample RS2799 also contained calcite and ankerite veins, which cut across the sedimentary layering. Most of the open pores identified in this thin section occurred in intercrystalline voids within the veins.

### *Well Log Results*

For the purposes of modeling the well logs, the modal composition of the rock strata was defined by the seven principal mineral phases: Fe-rich illite, chlorite, muscovite, albite, quartz, calcite, and ankerite. Since the geophysical logs could not distinguish between albite and quartz or between calcite and ankerite, these were grouped to form two model components, framework silicates and carbonates. Thin-section observations indicated that the ratio of calcite to ankerite was ~1.5, and EPMA analyses were used to fix the composition of the bulk carbonate (Table 4). Since the principal K-bearing phases were illite and muscovite (biotite being a minor constituent), we used equation 1 to model their volumetric abundance (Table 4). And since the principal Th-bearing phases were chlorite, illite, and to a lesser extent muscovite (Table 4; Schlumberger 1995), the volumetric abundance of chlorite was constrained by equation 2. Because the photoelectric cross-section is sensitive to minerals

TABLE 4 Petrophysical parameters utilized in forward-modeling of borehole geophysical data

| Phase | K(wt%) | Th(ppm) | $\rho$(g/cm$^3$) | $\rho$e(g/cm$^3$) | Pe | N$\phi$ |
|---|---|---|---|---|---|---|
| Illite | 7 | 16 | 2.90 | 2.87 | 3.61 | 15 |
| Chlorite | 0 | 47 | 2.60 | 2.61 | 2.53 | 36 |
| Muscovite | 8.3 | 0 | 2.82 | 2.80 | 2.40 | 12 |
| Carbonate | 0 | 0 | 2.80 | 2.79 | 5.31 | 0 |
| Albite | 0 | 0 | 2.62 | 2.60 | 1.68 | −1 |
| Quartz | 0 | 0 | 2.64 | 2.64 | 1.81 | −1 |
| Water | 0 | 0 | 1.00 | 1.11 | 0.36 | 100 |
| Gas | 0 | 0 | 0.22 | 0.09 | 0.11 | 45 |

$\rho e = \rho\ (2\sum n_i Z_i/A)$, where $Z_i$ is the atomic number of each atom present in the molecular formula for each phase, $n_i$ is the stoichiometric coefficient, and A is the molecular weight.

$Pe = \sum(n_i Z_i Pe_i)/\sum n_i Z_i$, where $Pe_i$ is the photoelectric absorption cross-section index for each element present in the molecular formula for each phase. The units are barns per electron.

N$\phi$ = apparent neutron porosity.

The following molecular formulas were utilized in calculating the $\rho$e and Pe for each phase: illite, $K_{1.5}Fe_{1.2}Al_{4.3}Si_{6.5}O_{20}(OH)_4$, where the Fe is assumed to be Fe(III); chlorite, $Mg_7Fe_{0.8}Al_{3.2}Si_{6.5}O_{20}(OH)_{16}$, where the Fe is assumed to be Fe(II); muscovite, $K_2Al_6Si_6O_{20}(OH)_4$; carbonate, $0.6CaCO_3 + 0.4Mg_{0.7}Fe_{0.3}CaC_2O_6$; albite, $NaAlSiO_3$; quartz, $SiO_2$; water, $H_2O$; gas, $CH_4$.

containing elements with high atomic numbers, such as Ca and Fe (Table 4), the amount of carbonate in the formation was constrained by equation 4. The volumetric abundance of sulfide was far too small to significantly affect the photoelectric log. The volumetric abundance of the framework silicates (albite + quartz) was constrained by equation 3, and the volumetric abundances of carbonate, illite, chlorite, and muscovite.

Across the sampling zone, the shale content (illite + chlorite + muscovite) averaged 40% by volume and ranged from 12% to 57% (Figure 3). The carbonate content averaged 35% by volume and ranged from 9% to 74% (Figure 3). The Fe concentration was estimated for the sedimentary strata by using the modal analyses derived from the petrophysical logs (Figure 3) and the Fe concentrations of the carbonate, chlorite, and illite (Table 4). These values were slightly varied until the estimated Fe concentrations matched those measured on the rotary sidewall cores. The samples RS2799, RS2794, and RS2793 were particularly useful in constraining the Fe concentrations of these three phases, because these samples exhibited various proportions of Fe and inorganic carbon. The wt% Fe averaged 2.9% and ranged from 0.9% to 6.4% across the sampling interval (Table 4). The Fe(III)/Fe was estimated for these strata by assuming that all the Fe in illite was Fe(III) (Weaver and Pollard 1973) and that all the Fe in chlorite and in carbonate was Fe(II). The model Fe(III)/Fe averaged 0.6 (range 0–0.9) (Figure 3). These general compositional variations are consistent with those determined by Van Houten (1965) for the chemical cycles of the Lockatong Formation, a lacustrine facies within the Triassic Newark Group of the Newark Basin that may be stratigraphically correlated with the Falling Creek Member of Taylorsville basin (P.E. Olsen, pers. comm., 1995).

RS2793, RS2794, and RS2799 were extracted from a 17-m-thick coarsening-upward unit. The shale content decreased from 57% to 24% from RS2799 to RS2793. The carbonate content decreased slightly from ~45% to 35% across this same interval. The modeled Fe concentration decreased substantially, from 5.4% to 1.6%, with a concomitant decrease in the Fe(III)/Fe, from 0.8 to 0.4. This model yielded an estimated value of 0.68 for the Fe(III)/Fe for the horizons sampled by RS2799 and RS2794, in close agreement with the measured values (Table 3).

For a formation temperature of 76°C (see following section) and an $R_{mf}$ of 1.13 ohm m, the SP and resistivity logs and equation 8 indicated that the formation water in the sampled horizons ranged from 0.77 to 0.80 wt% NaCl equivalent (Table 5). The formation resistivity of the strata that are the most clay-rich was ~1.395 ohm m. Substituting this value into equation 7 and utilizing the resistivity log and the volumetric fractions of illite, chlorite, and muscovite for $F_c$, we calculated that the water saturation values averaged 50% across the sampling interval (range 25–100%). The clay-rich strata yielded higher saturation values, consistent with capillary effects.

The matrix density calculated from equation 6 agreed well with the matrix densities determined from the sidewall cores. The fluid density was assumed to be a volumetric combination of brackish water and methane densities (Table 4). The resulting porosity, derived from equation 6, averaged 5% across the sampling zone, which is consistent with the average of measured values for the Falling Creek Member (Summa et al. 1989). The porosity ranged from <~1% to as high as 30% (Figure 6). The higher porosity values appeared at discrete horizons, where dipmeter readings suggested the presence of a fracture (Figures 3 and 5). The calculated porosity was in very good agreement with laboratory measurements for RS2794, but was significantly higher (3–4%) than the 0.5–1.5% experimental determination for RS2799. We interpret the higher calculated porosity to reflect a contribution from fracture porosity that was not present in the sample on which the porosity was determined. The shale-rich layers typically contained numerous mineralized fractures that were not present in the carbonate cemented siltstone.

**TABLE 5** Formation temperature estimates derived from temperature logs and bottom hole temperature (BHT) measurements, and salinity estimates derived from SP logs

| Well | Type | *T* (°C) | Depth (mbls) | Well | NaCl (wt%) | Depth (mbls) | Well | NaCl (wt%) | Depth (mbls) |
|---|---|---|---|---|---|---|---|---|---|
| Thorn | BHT | 33 | 772 | Thorn | 1.3 | 2616 | 2 | 1.3 | 733 |
| Hill 1 | BHT | 82–83 | 3093 | Hill 1 | 1.3 | 2619 | | 2.1 | 785 |
| | BHT | 31 | 772 | | 1.0 | 2637 | | 1.8 | 809 |
| | BHT | 79–80 | 3073 | | 1.0 | 2640 | | 1.3 | 834 |
| 2 | Log | 22.7 | 133 | | 1.0 | 2643 | | 1.1 | 873 |
| | Log | 26.7 | 367 | | 1.5 | 2662 | | 3.7 | 891 |
| | Log | 30 | 600 | | 1.0 | 2665 | | 4.5 | 913 |
| | Log | 32.5 | 667 | | 1.7 | 2686 | | 4.2 | 983 |
| | Log | 36.7 | 833 | | 0.8 | 2720 | | 3.9 | 1004 |
| | Log | 38.8 | 867 | | 0.8 | 2780 | | 3.5 | 1065 |
| | Log | 41.1 | 1133 | | 1.4 | 2738 | | 3.4 | 1101 |
| | Log | 46.6 | 1267 | | 1.4 | 2741 | | 3.2 | 1183 |
| | BHT | 57 | 1640 | | 0.8 | 2780 | | 2.6 | 1244 |
| 3 | Log | 20 | 133 | | 0.8 | 2786 | | 2.5 | 1326 |
| | Log | 23.3 | 300 | 1 | 0.2 | 91 | | 2.8 | 1326 |
| | Log | 24.7 | 433 | | 0.1 | 319 | | 3.5 | 1345 |
| | Log | 28.3 | 633 | | 0.2 | 365 | | 2.7 | 1411 |
| | BHT | 32 | 815 | | 0.2 | 520 | | 2.9 | 1463 |
| 4 | Log | 39.2 | 1067 | | 0.6 | 715 | | 1.9 | 1484 |
| | Log | 20.8 | 200 | | 0.6 | 751 | | 1.7 | 1509 |
| | Log | 24.4 | 400 | | 0.5 | 791 | | 1.9 | 1554 |
| | Log | 30 | 667 | | 2.4 | 812 | | 2.5 | 1597 |
| | Log | 33.3 | 800 | | 0.8 | 903 | | 2.3 | 1624 |
| | Log | 40.6 | 1067 | | 1.0 | 940 | 3 | 1.2 | 630 |
| | Log | 44.4 | 1233 | | 0.5 | 960 | | 1.2 | 657 |
| | Log | 51.7 | 1433 | | 0.9 | 1053 | | 3.7 | 681 |
| | BHT | 58 | 1667 | | 0.5 | 1141 | | 3.9 | 797 |
| 5 | Log | 18.9 | 167 | | 0.7 | 1226 | | 2.2 | 885 |
| | Log | 23.2 | 233 | | 0.7 | 1357 | | 3.5 | 928 |
| | Log | 25.6 | 367 | | 1.8 | 1390 | | 2.3 | 976 |
| | Log | 28.1 | 600 | | 0.5 | 1582 | 5 | 0.6 | 447 |
| | Log | 32.2 | 733 | | 0.4 | 1807 | | 0.9 | 493 |
| | BHT | 38 | 911 | | 0.5 | 2069 | | 0.7 | 563 |
| | Log | 42.3 | 1130 | | 0.4 | 2361 | | 0.6 | 593 |
| | Log | 45 | 1267 | | 0.5 | 2476 | | 0.7 | 618 |
| 6 | Log | 21.7 | 100 | | 0.9 | 2616 | | 1.1 | 760 |
| | Log | 24.4 | 367 | | 1.0 | 2753 | | 0.9 | 681 |
| | Log | 27.5 | 533 | | 0.7 | 2863 | | 1.2 | 721 |
| | Log | 28.8 | 600 | | 0.7 | 2975 | | 1.4 | 761 |
| | Log | 32.2 | 800 | 2 | 0.6 | 599 | | 1.6 | 785 |
| | Log | 36.1 | 1067 | | 0.7 | 611 | | 2.5 | 861 |
| | Log | 37.8 | 1187 | | 1.7 | 639 | | 2.4 | 934 |
| | BHT | 57 | 1668 | | 0.9 | 709 | | 1.3 | 1013 |

(*Continued on next page*)

TABLE 5 Formation temperature estimates derived from temperature logs and bottom hole temperature (BHT) measurements, and salinity estimates derived from SP logs (*Continued*)

| Well | Type | $T$ (°C) | Depth (mbls) | Well | NaCl (wt%) | Depth (mbls) | Well | NaCl (wt%) | Depth (mbls) |
|---|---|---|---|---|---|---|---|---|---|
| 7 | BHT | 38 | 1018 | 5 | 1.4 | 1028 | 6 | 3.6 | 1393 |
| | Log | 21.7 | 200 | | 1.5 | 1059 | | 3.8 | 1445 |
| | Log | 26.7 | 400 | | 1.2 | 1098 | 7 | 0.5 | 473 |
| | Log | 30.6 | 600 | | 2.2 | 1165 | | 0.1 | 502 |
| | Log | 38 | 1067 | | 1.8 | 1226 | | 0.2 | 572 |
| | Log | 53 | 1700 | | 1.7 | 1253 | | 0.4 | 601 |
| | | | | | 1.7 | 1272 | | 0.2 | 624 |
| | | | | | 1.9 | 1335 | | 0.1 | 806 |
| | | | | | 2.0 | 1384 | | 0.1 | 955 |
| | | | | | 1.8 | 1415 | | 0.2 | 1019 |
| | | | | 6 | 6.0 | 952 | | 0.1 | 1074 |
| | | | | | 6.0 | 983 | | 0.1 | 1262 |
| | | | | | 6.5 | 1071 | | 0.1 | 1323 |
| | | | | | 5.9 | 1104 | | 0.1 | 1369 |
| | | | | | 4.5 | 1214 | | 0.1 | 1393 |
| | | | | | 4.0 | 1332 | | 0.2 | 1512 |
| | | | | | 4.0 | 1351 | | 0.2 | 1554 |
| | | | | | | | | 0.1 | 1612 |

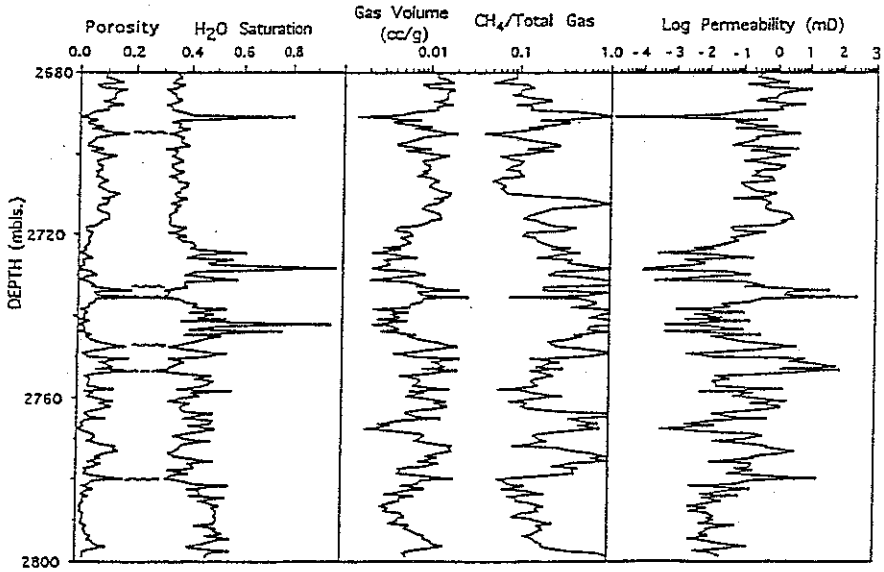


FIGURE 6 Variations in rock physical properties and fluid properties for microbial sampling zone of Thorn Hill 1 as determined from analyses of petrophysical logs. (Left) Porosity and water saturation; (middle) bulk gas volume (mL/g) and the fraction of $CH_4$ making up the gas volume; (right) permeability in milliDarcies. Location of fractures inferred from petrophysical logs are marked by dashed lines (as in Figure 3).

Calculated neutron porosity is sensitive to hydrogen content; in this case, it primarily reflected the chlorite abundance and the formation fluid and gas (Table 4). Equation 5 provided an additional constraint on the volume of gas-filled porosity in the section. The gas volumes calculated from equation 10 agreed well with the measured total gas logs. The relative hydrocarbon abundance in the gas phase ranged from 3% to 90% (average 25%) (Figure 5). The remainder of the gas was probably a combination of $N_2$, $CO_2$, and $H_2$, given the gas analyses results from other Triassic basins in the region (Marine 1979). The gas logs indicated that $CH_4$ made up 90–96% of the hydrocarbon gas.

For the strata between 2787 and 2793 mbls, the water saturation was fairly uniform at 65% (Figure 5). The gas concentration decreased upwards from the shale to the siltstone, reflecting the reduction in porosity, which, in turn, probably reflects the diminishing fracture density. The relative abundance of $CH_4$, however, remained the same.

Using 25 for the calibration constant, C, in equation 9, yielded calculated permeability values that matched those measured for sidewall cores RS2794 and RS2799. For this value of the constant, the calculated distribution of permeability values as a function of porosity was very similar to the measured values from cores of the Falling Creek Member taken in other parts of the basin (Fulton and Thomas 1987). The permeability averaged 3 mD across the sampling zone, which is also consistent with the average value of measured permeabilities for the Falling Creek Member (Summa et al. 1989). The calibration based upon the measured permeability values for RS2799 and RS2794, therefore, appears to be a good approximation. The permeability estimated for the fractured horizons was as high as 300 mD (Figure 6). Samples RS2793, RS2794, and RS2799 were collected from the middle of a 17-m-thick bed of uniformly low porosity (average 3%) and permeability (average 20 $\mu$D) bounded by narrow layers of higher porosity and permeability.

Comparison of the shallow, intermediate, and deep borehole resistivity profiles revealed variable degrees of penetration by the drilling mud filtrate into the formation across the sampling interval. Minor drilling fluid penetration was observed in the resistivity profiles for the more porous and permeable strata. Potentially, these horizons may have contained a greater indigenous microbial population, but they also had a thicker mud pack and greater filtrate contamination, precluding defensible microbial results. The lower portion of the 17-m-thick unit from which samples RS2793, RS2794, and RS2799 were extracted exhibited intermediate and deep borehole resistivities that were distinct from that of the shallow resistivity profile. This indicates that drilling mud filtrate penetration was minimal in the lower, clay-rich portion of this unit. In the upper portion of the same bed, the intermediate resistivity was higher than that of the shallow- and deep-resistivity profiles. This indicates that in the upper, clay-poor portion of this unit, the natural gas near the surface of the borehole was partially displaced by invading drilling mud filtrate.

### *Basin-Scale Borehole Analyses*

Corrected bottom hole temperatures and temperature logs from nearby gas exploration boreholes (Table 5) indicated that the geothermal gradient at Thorn Hill 1 could be closely fit with a purely conductive heat-transport model. Deflections in the temperature contours (Figure 7a) near the top of the Triassic sequence on the eastern side of the basin suggested that fluid advection may contribute to heat transport in that part of the basin. The borehole temperature data yielded an average geothermal gradient of 22 $\pm$ 2°C/km at Thorn Hill 1, which is consistent with regional heat flow measurements (Lambiase et al. 1980). From this gradient, we derived a temperature of 76 $\pm$ 6°C for 2800 mbls.

Pressure gradients derived from mud weights exhibited two significant departures from a hydrostatic depth gradient. Near the upper contact between the Doswell Formation and

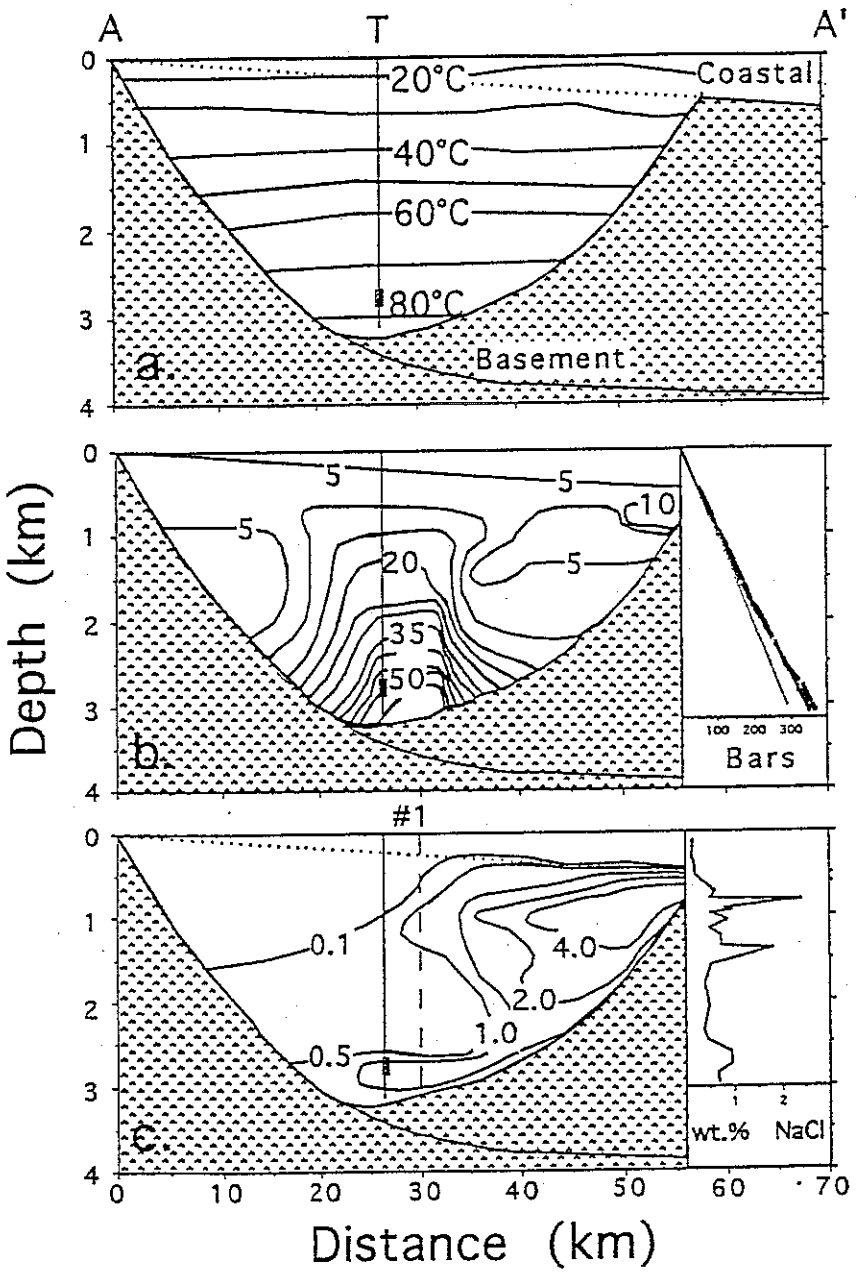


FIGURE 7 Line of cross-section is A–A' in Figure 1. Microbial sampling zones are indicated by the small black rectangles. (a) Contour plot of temperatures, based on bottom hole temperatures, borehole temperature profiles from exploration holes in Taylorsville Basin, and water temperatures of overlying aquifers. (b) Contour plot of pressures (in bars) exceeding hydrostatic values. Inset: Total pressures as a function of depth for Thorn Hill 1 (bold line) and Wilkins 1 (dashed line) compared with hydrostatic gradient corrected for salinity variations (solid line). All values are based on mud density in the boreholes and are presumed to slightly underestimate the fluid pressures of the formation. (c) Contour plot of salinity (wt% NaCl equivalent) for the Taylorsville Basin, based on analysis of SP profiles from boreholes. Inset: Vertical variation in salinity for Wilkin 1 (1 in Figure 1 and Table 5).

the Coastal Plain sequences, the formation fluid pressure was 0.4–1.0 MPa greater than predicted by a hydrostatic gradient (Figure 7b). This slight increase is similar in magnitude to that observed in the Dunbarton Basin and may reflect an osmotically induced hydraulic pressure differential (Marine and Fritz 1981), given the salinity gradient across this contact (see *Discussion*). Beneath this anomalous pressure zone, the mudweight estimated pressure followed a hydraulic gradient of 10–10.7 MPa/km until reaching ~2000 mbls, where the pressure gradient increased to 15 MPa/km (Figure 6b; inset). This transition coincided with the contact between the New Found Member and the Falling Creek Member and with an increase in the methane concentrations in the drilling mud (Tseng et al. 1995), thus suggesting that the increase in the pressure gradient was caused by gas pressure. At 2800 mbls the total fluid pressure was ~32 MPa.

The formation fluid salinity derived from SP logs and equation 8 varied across the basin (Table 5; Figure 7c). A steep salinity gradient was detected near the contact between the Doswell Formation and the overlying Coastal Plain sediments. In the center of the basin near Thorn Hill 1, the salinity of the formation fluid increased from 0.1 wt% NaCl equivalent in the Coastal Plain strata to 0.6–2.2 wt% within the first 150 to 400 m of the New Found Member (Figure 6c; inset). The salinity then decreased to a uniform 0.5 wt% in the upper Falling Creek Member and increased slightly to 0.8 wt% in the sampling zone. Within the Doswell Formation, the salinity gradient varied from 0.1–0.5 wt% NaCl equivalent on the western margin to 3–6 wt% NaCl equivalent on the eastern margin (Figure 7c). The cause of the elevated salinities in the eastern portion of the basin is unknown.

No direct determination of the Doswell Formation water pH is available. Studies of the formation water chemistry of nearby Triassic rift basins, Culpeper (Powell and Abe 1985), Durham (Bain and Brown 1981), and Dunbarton (Marine and Fritz 1981), however, indicate that the pH increased from 7.3 to 9.0 with increasing depth and with increasing salinity (up to 1.4 wt%). Given the depth and salinity of the sampled zone of Thorn Hill 1, an alkaline, brackish, formation water is highly probable.

## Discussion

### *Origins of Thorn Hill 1 Thermophilic Anaerobes*

The absence of culturable bacteria of any type, especially thermophilic anaerobes from the control sample enrichments, effectively rules out laboratory contamination as a source for the anaerobes found in the pared rotary sidewall cores. The drilling mud, however, with its large numbers of thermophilic anaerobes, represents the principal candidate for potential contamination of the sidewall cores. The amount of drilling mud present in the cores is constrained by the chemical and microbial tracers. Detectable PFT in the pared rotary sidewall cores (Table 2) indicates that limited chemical contamination of the cores by drilling mud filtrate did occur. The amount of contamination can be estimated from the following expression:

$$T_s = FT_c + (1 - F)T_{uc} \tag{11}$$

where $T_s$, $T_c$, and $T_{uc}$ are the trace concentrations in the pared sidewall core, the drilling mud, and the pristine rock formation, respectively, and F is the fractional mass of the contaminant relative to the sidewall core. Since perfluoromethylcyclohexane is not a naturally occurring compound, its concentration in the pristine rock formation is expected to be less than that of the control samples (4–9 ng/g in Table 2). $T_s$ ranges from 16 to 24 ng/g and $T_c$ is 790 ng/g (Table 2). With these values, equation 11 yields 1% to 2.5% for F. Given this amount of

mass transfer on to the sidewall core, the resulting percentage of microbial contamination is expressed by the following:

$$\%\text{Cont.} = 100[F/(1 - F)][(A_c/A_s) - 1] \quad (12)$$

where $A_c$ and $A_s$ represent the cells/g of thermophilic anaerobes cultured from the drilling mud and the pared sidewall core, respectively. For the cultured DIRB, $A_s$ ranged from 1 (RS2799) to $10^4$ cells/g (RS2793), and $A_c$ was $10^5$ cells/g (Table 2). The estimated contamination level is 13–25% for RS2793; for RS2799, it is >100%. The latter calculation indicates that the number of thermophilic bacteria recovered in the core is less than would be indicated by the tracer concentration. This incongruity may result from the migration of the PFT from the mud into the unsaturated rock at a pace greater than microbial transport (McKinley and Colwell 1996).

The PLFA concentrations indicate that the bacterial biomass of the drilling mud is 12 times that of the pared rotary sidewall cores (Table 2). The normalized PLFA profiles for the drilling mud were statistically distinct from that of the pared sidewall cores (Lehman et al. 1995). The fractional abundance of 16:1w7c and 18:1w7c were higher in the drilling mud sample (3 and 5 mol%, respectively) than in the pared rotary sidewall core (<0.5 and 2 mol%). These acids are typical of gram-negative heterotrophic bacteria and account for a large portion of the PLFA of the make-up water (24 and 22 mol%, respectively). Using these two fatty acids as our tracers and correcting for the total concentration of PLFA, we estimated the mass fraction of drilling mud contamination was 0.2–2.4%, similar to that determined from PFT analyses. The concentration of *anteiso*-PLFA in the drilling mud is also higher than that of the rotary sidewall core (3 vs 1 mol%) but is not present in the make-up water. The total fatty acids of gram-positive bacteria are largely in *anteiso* configurations and, given the phylogenetic correlation of the cultured strains with gram-positive bacteria, are most likely the signature of these thermophilic anaerobic bacteria. Correcting for the total PLFA concentration and utilizing equation 12, we estimated the percentage of contamination of the sidewall cores from the drilling mud ranged from 7% to 83%. This represents an improvement over the PFT constraints but still is not very reassuring.

The MPN determinations (Table 2) provide a greater level of confidence that the bacterial contamination of the pared rotary sidewall cores is minimal. The drilling mud samples contained aerobic microorganisms (>$10^6$ cells/g) as well as thermophilic anaerobes ($10^2$–$10^5$ cells/g). Similar concentrations of aerobic and anaerobic bacteria were found in the percussion cores (Table 2). Aerobes were not found in the rotary sidewall cores, however, where 1–$10^4$ thermophilic anaerobe cells/g of sediment were detected. This difference was confirmed by the aerobic CLPPs, which registered no response from the pared rotary sidewall cores, but did from the drilling mud and percussion sidewall cores (Table 2 and Lehman et al. 1995). The absence of an aerobic reaction in the pared rotary sidewall cores cannot be attributed to processing in the anaerobic glove bag, because the percussion and rotary sidewall cores were treated in the same manner.

If we assume that the rock environment provides for only obligate anaerobes, then the CFU/g for aerobic bacterica represents the tracer concentration and the $T_{uc}$ in equation 11 is zero. Since <0.3 aerobic cells/g were present in the pared rotary sidewall cores (Table 2), the mass fraction of bacteria contributed by the drilling mud contamination is $3 \times 10^{-5}$%. Given $10^5$ cells/g for DIRB in the drilling mud, equation 12 indicates that, for those cores bearing only 1 DIRB cell/gram (RS2799), the contamination level is on the order of 3% and, for those cores containing $10^4$ cells/g of DIRB (RS2793), the contamination level is $<3 \times 10^{-4}$%. Similar calculations for the SRB enrichments yield contamination levels of

$<3 \times 10^{-3}$%. These estimates indicate that if the culturable thermophilic anaerobes had entered the cores with the drilling mud filtrate, then culturable aerobes should have also been present and in greater abundance. The lower abundance of aerobes in the rotary sidewall cores cannot be attributed to preferential selection for anaerobes during sample processing, because methanogenic populations of $10^2$ cells/g were detected in the drilling mud and the percussion sidewall cores but not in the rotary sidewall cores (Table 2). Interpreted in this manner, the CFU and MPN data indicate that the anaerobic bacteria grown from the rotary sidewall cores were indigenous to the Falling Creek Member and not the result of drilling mud contamination.

Further evidence for their autochthonous nature comes from the following physiological characteristics of isolates derived from the anaerobic enrichments:

1. A dissimilatory Mn(IV)- and Fe(III)-reducing bacterium (DIRB) from RS2799 exhibited growth from 38.7 to 65.9°C (at 1 bar pressure), from a pH of 6.5 to 8.5, and from a salinity of 0.5 to 11.7 wt% NaCl equivalent (Boone et al. 1995). This strain could utilize either formate or $H_2$ as an electron donor, but not acetate, and could ferment glucose. The temperature range for this strain exhibits little pressure sensitivity up to 50 MPa (Delwiche et al. 1996).
2. An Fe-reducing strain, TOR 39 (Zhang et al. 1996) from RS2794, grew at temperatures of 50–70°C and at NaCl concentrations of 0.1–5.0 wt%. A magnetite-producing bacterium exhibited growth between 45 and 75°C (S.V. Liu et al. 1997). Other cultures grew at neutral to mildly alkaline pH (6.8–8.5), tolerated 4–11 wt% NaCl, and exhibited temperature optima >55°C, with many growing at 75°C.

These physiological traits are less consistent with the measured 40°C temperature, 0.1 wt% NaCl, and the 8.5–9.5 pH of the drilling mud than with the 76°C formation temperature and 0.8 wt% NaCl formation fluid salinity estimated from geophysical logs. Their pH growth ranges are also more consistent with the pH of 7–9 reported for deep groundwater of adjacent Triassic basins (Powell and Abe 1985; Bain and Brown 1981; Marine and Fritz 1981).

Another line of supporting evidence comes from the Hg porosimetry data. The 0.04-$\mu$m maximum pore-throat diameter (Figure 4a) is smaller than the 0.1–0.4-$\mu$m diameter of "ultramicrobacteria" that have been observed in marine samples in response to survival stress (Torella and Morita 1981). Such a small pore size would exclude even the smallest bacterial cells entrained in the drilling mud filtrate.

A final line of evidence that argues against a surface origin for the thermophilic anaerobes cultured from the cores is based on the variation in the drilling mud microbial community structure as a function of depth. These variations could have been caused either by preferential selection of bacteria in the drilling mud with increasing depth or inoculation of the drilling mud by subsurface bacteria present in the formation. The following observations suggest that the latter was the case:

1. The depth where saline-tolerant, thermophilic-fermenting, and sulfate-reducing bacteria and methanogens first appeared coincided with penetration of the low-permeability Falling Creek Member, intersection of the diabase intrusion, a rapid increase in formation pressure, and a sudden rise in the methane gas concentrations. These data suggest that drilling had entered a more hydrologically isolated section of the Doswell Formation. Intriguingly, aerobic thermophiles were enriched in drilling mud samples at shallower depths, but not at the depths where the thermophilic anaerobes began to appear.
2. At this depth the formation fluid salinity increased to 0.5 wt% NaCl (Figure 3c) and the formation temperature reached 60–65°C. The drilling mud salinity and

temperature, however, remained at 0.1 wt% NaCl and 40°C, varying little as a function of depth.

3. Anaerobic thermophiles were not detected in any of the enrichments of the unused drilling mud components (<1 cell/g). Methanogens, sulfate-reducing bacteria, and Fe-reducing bacteria have been reported in the groundwater of the aquifer utilized for make-up water (Chapelle et al. 1987; Chapelle and Lovley 1990), but only mesophilic varieties have been reported to date (Lovley et al. 1990).

Because the shift in the drilling mud microbial community structure correlated with changes in the formation environment, rather than with any change in the drilling mud environment, the drilling mud was probably inoculated by bacteria from the formation at this depth. Therefore, many, if not all, of the thermophilic, saline-tolerant, anaerobic bacteria found in the deeper drilling mud samples were probably derived from strata within the Falling Creek Member. Since the near-surface drilling muds contained <1 thermophilic, anaerobic cell/g and the deep subsurface drilling muds contained up to $10^2$ thermophilic, anaerobic cells/g, the probability that the thermophilic anaerobes are a surface contaminant becomes even less than the above estimates.

The results of phylogenetic characterization based on analysis of the 16S ribosomal RNA indicated that one of the DIRB represents a new species of *Bacillus*, *Bacillus infernus* sp. nov. (Boone et al. 1995). Two other strains of DIRB appear to represent new species of *Thermoanaerobacter* (S.V. Liu et al. 1997). Six strains of thermophilic SRB were also isolated from the pared rotary sidewall cores (Y. Liu et al., unpublished). These six SRB strains were phylogenetically indistinguishable and represent a new species of *Desulfotomaculum* (Y. Liu et al., unpublished). All strains fall within the gram-positive group of the eubacteria. The fact that these isolates represent new species is not necessarily evidence that they must be indigenous to the deep subsurface of Taylorsville Basin, given the small percentage of all Bacteria and Archea that have been phylogenetically classified (for example, see Torsvik et al. 1990). However, new species of bacteria are more likely to be encountered in deep subsurface settings that have been sequestered from the surface for geologically significant periods of time.

### *Geomicrobiology of the Falling Creek Member*

Petrological analyses of the sidewall cores and cuttings and the modeling of the resistivity log indicate that this portion of the Falling Creek Member represents cyclic lacustrine deposits, similar to those observed in the Triassic strata of the Newark basin of New Jersey and of the Culpeper basin in central Virginia (Olsen 1986; Smoot and Robinson 1988). The Falling Creek Member cyclic deposits are ~10–20 m thick (Figure 3) and are probably related to the transgression and regression of a lake in response to climatic changes (Olsen 1986). During transgressive stages, the clay, fine-grained Fe oxides and carbonate content increased, and during regressive stages, the silt content (albite, quartz, and muscovite) increased. During thermal maturation of the strata, the clay and silt were transformed into siltstone and shale, and the clay minerals formed Fe(III)-rich illite.

The MPN estimates (Table 2) indicated that greater concentrations of the DIRB were found in the siltstone layers (RS2793) than in the shale layers (RS2799), even though the Fe concentration was greater in the shale layers (Table 3). This apparent incongruity may be explained by the petrographic observation that, in the siltstone layers, the illite lines the visible pores. If the Fe(III) in the clay structure is bioavailable for reduction, then the DIRB would have ready access to the Fe(III). Recent evidence for the microbial reduction of ferric iron in smectite by *Shewanella putrefaciens* (Kostka et al. 1996) encourages this

speculation. On the other hand, in the highly compacted, organic-rich shale, the visible pore space is restricted primarily to fractures. Because these fractures are lined with calcite, sulfide, and quartz, the Fe(III)-bearing illite would not be as available to the DIRB as in the siltstone.

The fractures can provide an enhanced flux of soluble electron acceptors, such as sulfate and bicarbonate. This might explain why the SRB are more abundant in the shale strata than in the siltstone layers. The presence of late-stage, framboidal pyrite is arguably consistent with occurrence of SRB. The sulfate concentration of the Falling Creek Member is unknown, but sulfate is present in the groundwater of other Triassic basins in the region (Marine and Fritz 1981; Bain and Brown 1981; Powell and Abe 1985).

Although the concentration of dissolved organic acids in the formation water is unknown, the presence of abundant organic matter in the sedimentary rock and hydrocarbons in the gas phase is consistent with the presence of heterotrophic bacteria in the enrichments. The occurrence of $H_2$-utilizing bacteria also is not surprising, given the likely presence of $H_2$ in this formation at concentrations similar to the high levels of dissolved $H_2$ observed in the groundwater of other Triassic basins (Marine 1979). In this formation, $H_2$ may be generated as a fermentation end product or by radiolytic reactions of $H_2O$ with alpha particles emitted by U (Hoffman 1992). Indeed, high levels of U were observed at discrete horizons within the Falling Creek Member adjacent to the sampled horizons (Tseng et al. 1995).

The elevated concentrations of U, Th, and K in the Falling Creek Member also indicate that the culturable bacteria recovered from the samples were probably engaged in a minimal level of metabolic activity that was sufficient to repair the DNA damage induced by alpha, beta, and gamma radiation. Without this activity, the genomes responsible for successful regeneration of the DNA would be irreversibly destroyed. The dosage rate of the gamma radiation, which has the greatest penetration distance, can be derived from the spontaneous gamma ray log by the following relationship:

$$R = 1.27 \times 10^{-12}\ \text{GAPI} \tag{13}$$

where R is the dosage rate in Grays/g s and GAPI is the gamma ray flux in API units (equivalent to 60 ng/ton of Ra) measured by the spontaneous gamma ray logging tool. The GAPI ranged from 100 to 200 between 2790 and 2800 mbls, corresponding to $1.3 \times 10^{-10}$ to $2.5 \times 10^{-10}$ Grays/g s or $4 \times 10^{-3}$ to $8 \times 10^{-3}$ Grays/g yr. For bacterial strains collected from the subsurface aquifers beneath Savannah River, Georgia, 22–120 Grays dosage was required to kill 63% of the total population (Arrage et al. 1993) compared with 3000 Grays for *Deinococcus radiodurans*. For spores of *Bacillus megaterium*, ~500 Grays was required to achieve similar lethal dosages (Powers 1983). The radiosensitivity of subsurface isolates from the Taylorsville Basin have not been determined, but if they fell in the range of 22–3000 Grays, then the majority of viable cells in the Falling Creek Member would experience lethal exposure after ~6000 to 750,000 years. This calculation suggests that the culturable bacteria could not have survived for millions of years in a spore and that the SRB and DIRB were therefore biochemically active, albeit at barely detectable levels.

SRB and DIRB apparently coexist in RS2799 and are not separated into distinct zones by competition for $H_2$ and acetate, as was observed to be the case for shallower, premeable aquifers (Chapelle and Lovley 1992). In this low-porosity, low-permeability formation, SRB and DIRB are likely to occur in separate microhabitats, with DIRB existing in proximity to a solid-phase Fe(III) source. The low-permeability and small pore throat structure would severely restrict the migration of a bacterial cell to other solid-phase Fe(III) once its immediate source is depleted. Consequently, a mobile electron donor species, such as $H_2$ or acetate, would be required, and lack of the latter would limit DIRB metabolic activity. Only

through electron transport by dissolved humic compounds, as has recently been reported (Lovley et al. 1996), could the DIRB defeat the Fe(III) limitation imposed on them by the physical constraints of the formation. Whether or not this mechanism is important in the deep subsurface has yet to be determined.

### *Comparisons With Other Subsurface Microbial Sites*

In water-saturated sediments where microorganisms are active, the phospholipids of nonviable bacteria are rapidly dephosphorolated by phospholipases (White et al. 1979). Consequently, the concentration of PLFA can be interpreted as a measure of viable biomass. The total PLFA in sample RS2799 was 16 pmol/g (Table 2). This value corresponds to $4 \times 10^5$ cells/g, obtained by using the conversion factor of $(2.5 \pm 2) \times 10^4$ cells/pmol. This conversion factor is derived from a starved cellular mass of $(1.7 \pm 1.1) \times 10^{-13}$ g/cell (Balkwill et al. 1988) and therefore is an appropriate conversion factor to apply to these PLFA concentrations. Even considering the complexities of converting chemical biomarkers to numbers of cells in a diverse in situ community (White et al. 1996), the PLFA estimate of the cellular density is indisputably much higher than the 1 cell/g derived from the MPN enumeration method (Table 2). This discrepancy could arguably reflect either our inability to culture 99.98% of the viable microorganisms in the rock samples or centimeter-scale heterogeneity in the microbial biomass of the pared sidewall cores.

Alternatively, could the 65% water saturation level of the Falling Creek Member inhibit the rate of phospholipid degradation? Because most of the porosity occurs as submicrometer-diameter pores, capillary forces will trap this liquid water within these pores, leaving the larger pores occupied by the bacteria with no more than a thin film of liquid water coating the mineral surfaces. All of the pores may have been occupied by water originally, but if the $CH_4$ partial pressure increased with time, then the $H_2O$-filled pores containing viable bacteria may have become replaced by $CH_4$. Because of the submicrometer pore throat sizes, moreover, the viable bacteria would be unable to move out of the pore, and viable bacteria occupying nearby $H_2O$-filled pores would be unable to access the bacteria trapped in the $CH_4$-filled pore. The rates of dephosphorylation of the PFLAs and of the depurination and depyrimidation of DNA of a cell that expires or lyses in a $CH_4$-filled pore are probably less than those for an $H_2O$-filled pore, although how much less is not known. The discrepancy between the culturable cell density and the cell density estimated by PFLA concentrations also could not be verified by direct counts of cells with relatively intact DNA because the small sample size and low biomass precluded statistically valid estimates. Nevertheless, a similar environment is believed to have contributed to the survival of bacterial DNA, and presumably phospholipids, in ancient amber deposits (DeSalle et al. 1992).

Comparisons between the PLFA-estimated biomass and the MPN-estimated biomass has been published for other subsurface environments. Kieft et al. (1995) and Fredrickson et al. (1995) reported cell counts of $10^5$ cells/g by using acridine orange and PLFA concentrations of 0.5–45 pmol/g for rock samples collected at a depth of 180 mbls from Miocene Age lacustrine sediments of the Ringold Formation of southeastern Washington. Intriguingly, these biomass concentrations are similar to the much deeper and far more ancient lacustrine Falling Creek Member. The concentrations of organic carbon, carbonate carbon, and Fe are greater in the Falling Creek Member than in the Ringold Formation, perhaps reflecting differing climates at the time of deposition. The permeabilities of the lacustrine Ringold Formation ranged from 1 to 500 $\mu$D, similar to those of the Falling Creek Member. Ringold Formation samples with greater permeability typically yielded higher PLFA concentrations. The MPNs from the same samples ranged up to $10^5$ cells/g and were dominated

by mesophilic fermenters and DIRB (McKinley et al. 1997). A much larger portion of the bacterial cells detected in the Ringold Formation could be cultured, therefore, than was true for those from the Falling Creek Member. Whether this difference is related to the lower water saturation of the Falling Creek Member is uncertain, but interestingly, in the vadose zone immediately overlying the Ringold Formation, MPN values were near or below the detection limit (Fredrickson et al. 1993). The more-recalcitrant nature of the organic carbon and Fe(III) mineral phases in the Falling Creek Member may also contribute to the lower concentrations of culturable bacteria detected in this formation.

Fredrickson et al. (1997) reported PLFA concentrations of 0.4–31.9 pmol/g for rock samples collected at 200 mbls from Cretaceous Age marine Mancos Shale and Dakota Sandstone formations of northeastern New Mexico. These values are also similar to that of the Falling Creek Member. Although this concentration corresponded to $10^4$–$10^6$ cells/g (Balkwill et al. 1988), enrichments typically yielded barely detectable growth (<1 cell/g). The hydraulic conductivities of the rock samples are comparable with those of the Falling Creek Member and the Ringold Formation. Unlike the Falling Creek Member, however, the Mancos and Dakota Formations are fully water-saturated. The low concentrations of bacteria that could be cultured from the latter were attributed to electron donor limitations mitigated by the low permeability (Krumholz et al. 1997).

The huge disparity between the PLFA concentrations observed in the samples of the Falling Creek Member and the number of cells that can be cultured from those samples has been observed at other subsurface sites, but its cause remains elusive.

## Conclusions

Multiple lines of evidence indicate that the microorganisms cultured from rock cores collected from a natural gas–bearing formation, 2800 mbls in Taylorsville Basin, are indigenous and do not represent contamination from the drilling process. The culturable microbial community was composed primarily of thermophilic, saline-tolerant, anaerobic heterotrophs, DIRB, and SRB and was distinct from that of the surface soils, overlying Coastal Plain aquifers, and drilling fluids. The optimal growth temperatures and salinity tolerances and the electron donor and acceptor capabilities of isolated members of the community are consistent with formation temperature (76°C), fluid salinity (0.8 wt% NaCl equivalent), and geochemistry. Other, more tentative conclusions can be drawn from our combined knowledge of the geology, geochemistry, and geomicrobiology of the formation. For example, DIRB may have participated in the reduction of the Fe(III) present in diagenetic illite, and SRB may have been responsible for the late-stage framboidal pyrite. Given the elevated concentrations of U and K in the formation, the bacteria may have engaged in a level of metabolic activity sufficient to repair DNA damaged by radiation within the time frame of 10 kyr. They must perform this activity while confined within the rare (0.04% porosity) micrometer-size intercrystalline pores delimited by late diagenetic cements in siltstone and within cross-cutting, mineralized fractures in shale filled with brackish, alkaline water. The bacteria must also be barotolerant or barophilic, given the 32-MPa ambient pressure.

Finally, the biomass estimated from PLFA is comparable with that of much-shallower and younger subsurface environments. Assuming that phospholipid turnover occurred in this environment, the conversion of PLFA to cell numbers revealed that <0.1% of the cells containing PLFA could be cultured. This small proportion of culturable cells has been observed for other subsurface sites and may reflect either our inability to grow most of the cells in the laboratories or a slow growth rate from the turnover of the PLFA of nonviable cells trapped within the highly impermeable rock, or both.

## References

Alger RP, Ramer LL, Hoyle WR, Tixier MP. 1963. Formation density log applications in liquid-filled holes. J Petrol Tech 15:312–332.

Arrage AA, Phelps TJ, Benoit RE, Palumbo AV, White DC. 1993. Bacterial sensitivity to UV light as a model for ionizing radiation resistance. J Microbiol Methods 18:127–136.

ASTM. 1987. Annual book of ASTM standards, section 11, water and environmental technology, D513-Method G, p 422–424.

Balkwill DL. 1988. Numbers, diversity, and morphological characteristics of aerobic, chemoheterotrophic bacteria in deep subsurface sediments from a site in South Carolina. Geomicrobiology 7:33–52.

Balkwill DL, Ghiorse WC. 1985. Characterization of subsurface bacteria associated with two shallow aquifers in Oklahoma. Appl Environ Microbiol 50:580–588.

Balkwill DL, Leach FR, Wilson JT, McNabb JF, White DC. 1988. Equivalence of microbial biomass measures based on membrane lipid and cell wall components, adenosine triphosphate, and direct counts in subsurface aquifer sediments. Microb Ecol 16:73–84.

Bain GL, Brown CE. 1981. Evaluation of the Durham Triassic Basin of North Carolina and techniques used to characterize its waste-storage potential. US Geol Surv Open-File Rep 80-1295:132p.

Bastin ES. 1926. The presence of sulphate-reducing bacteria in oil-field waters. Science 63:21–24.

Boone DR, Liu Y, Zhao Z, Balkwill DL, Drake GR, Stevens TO, Aldrich HC. 1995. Bacillus infernus sp. nov. Fe(III)- and Mn(IV)-reducing anaerobe from the deep terrestrial subsurface. Int J System Bacteriol 45:441–448.

Chapelle FH, Lovley DR. 1990. Rates of microbial metabolism in deep coastal plain aquifers. Appl Environ Microb 56:1865–1874.

Chapelle FH, Lovley DR. 1992. Competitive exclusion of sulfate reduction by Fe(III)-reducing bacteria: a mechanism for producing discrete zones of high-iron ground water. Ground water 30:29–36.

Chapelle FH, Zelibor JL Jr, Grimes DJ, Knobel LL. 1987. Bacteria in deep coastal plain sediments of Maryland: a possible source of $CO_2$ to groundwater. Water Resour Res 23:1625–1632.

Coates GR, Dumanoir JL. 1974. A new approach to improved log derived permeability. Log Anal 15:17–31.

Collinson DW. 1983. Methods in rock magnetism and palaeomagnetism. New York: Chapman and Hall, 503 pp.

Cornet B, Olsen PE. 1990. Early to Middle Carnian (Triassic) flora and fauna of the Richmond and Taylorsville Basins, Virginia and Maryland, U.S.A. Martinsville, VA: Virginia Museum Natl Hist Guidebook 1:83.

Delwiche M, Colwell FS, Tseng H-Y, Gao G, Onstott TC. 1996. Pressure and temperature adaptation of a bacterium recovered from 2.8 kilometers beneath the surface of the earth. Abstr. 96th Ann Mtg Am Soc Microbiol, New Orleans.

DeSalle R, Gatesy J, Wheeler W, Grimaldi D. 1992. DNA sequences from a fossil termite in Oligo-Miocene amber and their phylogenetic implications. Science 257:1933–1936.

Eaton AD, Clesceri LS, Greenberg AE. 1995. 4500-Norg. In Standard Methods for the examination of water and wastewater, 19th ed. Philadelphia, PA: American Public Health Association, American Water Works Association, Water Pollution Control Federation, 4-91–4-95.

Fredrickson JK, Balkwill DL, Zachara JM, Li S-MW, Brockman FJ, Simmons MA. 1991. Physiological diversity and distributions of heterotrophic bacteria in deep Cretaceous sediments of the Atlantic Coastal Plain. Appl Environ Microbio 57:402–411.

Fredrickson JK, Brockman FJ, Bjornstad BN, Long PE, Li SW, McKinley JP, Wright JV, ConCa JL, Kieft TL, Balkwill DL. 1993. Microbiological characteristics of pristine and contaminated deep vadose sediments from an arid region. Geomicrobiol J 11:95–107.

Fredrickson JK, McKinley JP, Bjornstad BN, Long PE, Ringelberg DB, White DC, Krumholz LR, Suflita JM, Colwell FS, Lehman RM, Phelps TJ, Onstott TC. 1997. Pore-size constraints on the activity and survival of subsurface bacteria in a late Cretaceous shale-sandstone sequence, northwestern New Mexico. Geomicrobiol J 14:183–202.

Fredrickson JK, McKinley JP, Nierzwicki-Bauer SA, White DC, Ringelberg DB, Rawson SA, Li S-M, Brockman FJ, Bjornstad BN. 1995. Microbial community structure and biogeochemistry of Miocene subsurface sediment: implications for long-term microbial survival. Mol Ecol 4:619–626.

Fulton SM, Thomas AR. 1987. Diagenesis and aspects of porosity in Triassic arenites, Taylorsville Basin, Virginia. Texaco Inc. New Orleans Geol Lab, 141 pp.

Gondouin M, Tixier MP, Simard GL. 1986. An experimental study of the influence of the chemical composition of electrolytes on the S.P. curve in openhole well logging. SPE Reprint Series 21, p 59–73. Society of Petroleum Engineers of the American Institute of Mining, Metallurgical and Petroleum Engineers, Richardson TX.

Gurevich MS. 1962. The role of microorganisms in producing the chemical composition of ground water. In: SI Kuznetsov, editor. Geologic activity of microorganisms. [Trans (Trudy) Inst Microbiol 9:65–75], New York: Consultants Bureau.

Hoffman BA. 1992. Isolated reduction phenomena in red beds: a result of porewater radiolysis? In: YK Kharaka, AS Maest, editors. Water-rock interaction. Rotterdam/Brookfield: AA Balkema. p 503–506.

Kieft TL, Fredrickson JK, McKinley JP, Bjornstad BN, Rawson SA, Phelps TJ, Brockman FJ, Pfiffner SM. 1995. Microbiological comparisons within and across contiguous lacustrine, paleosol, and fluvial subsurface sediments. Appl Environ Micro 61:749–757.

Kostka JE, Stucki JW, Nealson KH, Wu J. 1996. Reduction of structural Fe(III) in smectite by a pure culture of Shewanella putrefaciens strain MR-1. Clays Clay Minerals 44:522–529.

Krumholz LR, McKinley JP, Ulrich GA, Suflita JM. 1997. Confined subsurface microbial communities in Cretaceous rock. Nature 386:64–66.

Lachenbruch AH, Brewer MC. 1959. Dissipation of the temperature effect in drilling a well in Arctic Alaska. US Geol Surv Bull N1083-C:73–109.

Lambiase JJ, Dashevsky SS, Costain JK, Gleason RJ, McClung WS. 1980. Moderate-temperature geothermal resource potential of the Northern Atlantic Coastal Plain. Geology 8:447–449.

Lehman RM, Colwell FS, Ringelberg DB, White DC. 1995. Combined microbial community-level analyses for quality assurance of terrestrial subsurface cores. J Microbiol Methods 22:263–281.

L'Haridon S, Reysenbach AL, Glenat P, Prieur D, Jeanthon C. 1995. Hot subterranean biosphere in a continental oil reservoir. Nature 377:223–224.

Liu SV, Zhou J, Zhang C, Cole DR, Gajdarziska-Josifovska M, Phelps TJ. 1997. Thermophilic Fe (III)-reducing bacteria from the deep subsurface: the evolutionary implications. Science 277: 1106–1109.

Liu Y, Karnauchow TM, Jarrell KF, Balkwill DL, Drake GR, Ringelberg D, Clarno R, Boone DR. 1997. Description of two new thermophilic species of Desulfotomaculum, Desulfotomaculum putei sp. nov. from a deep terrestrial subsurface and Desulfotomaculum luciae sp. nov. from a hot spring. Int J Syst Bacteriol (submitted).

Lovley DR, Chapelle FH, Phillips EJP. 1990. Fe(III)-reducing bacteria in deeply buried sediments of the Atlantic Coastal Plain. Geology 18:954–957.

Lovley DR, Coates JD, Blunt-Harris EL, Phillips EJP, Woodward JC. 1996. Humic substances as electron acceptors for microbial respiration. Nature 382:445–448.

Lowrie W, Ogg JG. 1986. A magnetic polarity time scale for the Early Cretaceous and Late Jurassic. Earth Planet Sci Lett 76:341–349.

Marine IW. 1979. The use of naturally occurring helium to estimate groundwater velocities for studies of geologic storage of radioactive waste. Water Resour Res 15:1130–1136.

Marine IW, Fritz SJ. 1981. Osmotic model to explain anomalous hydraulic heads. Water Resour Res 17:73–82.

McKinley JP, Colwell FS. 1996. Application of perfluorocarbon tracers to microbial sampling in subsurface environments using mud-rotary and air-rotary drilling techniques. J Microbiol Methods 26:1–9.

McKinley JP, Stevens TO, Fredrickson JK, Zachara JM, Colwell FS, Wagnon KB, Smith SC, Rawson SA, Bjornstad BN. 1997. Biogeochemistry of anaerobic lacustrine and paleosol sediments within an aerobic unconfined aquifer. Geomicrobiol J 14:23–39.

Milici RC, Bayer KC, Pappano PA, Costain JK, Coruh C, Nolde JE. 1991. Preliminary geologic

section across the buried part of the Taylorsville Basin, Essex and Caroline Counties, Virginia. Vir Div Min Res Open-File Rep 91-1:31 p.

Olsen PE. 1986. A 40-million-year lake record of Early Mesozoic orbital climatic forcing. Science 234:842–843.

Onstott TC, Balkwill DL, Boone DR, Colwell FS, Griffin T, Kieft TL, Lehman RM, McKinley JP, Nierzwicki-Bauer S, Tseng HY, Gao G, Phelps TJ, Ringelberg D, Russell B, Stevens TO, White DC, Wobber FJ. 1994. D.O.E. seeks origin of deep subsurface bacteria. EOS 75:385, 395–396.

Phelps TJ, Fliermans CB, Garland TR, Pfiffner SM, White DC. 1989. Methods for recovery of deep terrestrial subsurface sediments for microbiological studies. J Microbiol Methods 9:267–279.

Powell JD, Abe JM. 1985. Availability and quality of groundwater in the piedmont province of Virginia. US Geol Surv Water Resour Invest Rep 85-4235:33 p.

Powers EL. 1983. Physical determinants of radiation sensitivity in bacterial spores. Adv Space Res 3:73–78.

Robbins EI, Perry WJ Jr., Doyle JA. 1975. Palynological and stratigraphic investigations of four deep wells in the Salisbury Embayment of the Atlantic Coastal Plain. US Geol Surv Open File Report 75-307.

Rueter P, Rabus R, Wilkes H, Aeckersberg F, Rainey FA, Jannasch HW, Widdel F. 1994. Anaerobic oxidation of hydrocarbons in crude oil by new types of sulphate-reducing bacteria. Nature 372:455–458.

Schlumberger Wireline and Testing. 1995. Log interpretation charts. Houston, TX: Schlumberger.

Smoot JP, Robinson GR Jr. 1988. Sedimentology of stratabound base-metal occurrences in the Newark Supergroup. In: AJ Froelich, GR Robinson Jr, editors. Studies of the early Mesozoic basins of the Eastern United States. US Geol Surv Bull 1776:356–376.

Stetter KO, Huber R, Blochl E, Kurr M, Eden RD, Fielder M, Cash H, Vance L. 1993. Hyperthermophilic Archaea are thriving in deep North Sea and Alaskan oil reservoirs. Nature 365:743–745.

Stevens TO, McKinley JP. 1995. Lithoautotrophic microbial ecosystems in deep basalt aquifers. Science 270:450–454.

Stevens TO, McKinley JP, Fredrickson JK. 1993. Bacteria associated with deep, alkaline, anaerobic groundwaters in southeast Washington. Microb Ecol 25:35–50.

Summa LL, Paxton ST, Jennette DC, Burgess CF, Elledge BS, Klett TR, Hiemann MH. 1989. Regional reservoir quality study of Triassic sandstones from the Taylorsville Basin. Eastern U.S. Mesozoic Rift System. Exploration Res Appl Rep 20 pp., Exxon Production Research Co, Houston, TX.

Swanson BF. 1981. A simple correlation between permeabilities and mercury capillary pressures. J Petrol Technol December:2488–2504.

Szewzyk U, Szewzyk R, Stenström T-A. 1994. Thermophilic, anaerobic bacteria isolated from a deep borehole in granite in Sweden. Proc Natl Acad Sci USA 91:1810–1813.

Torella F, Morita RY. 1981. Microcultural study of bacterial size changes and microcolony formation by heterotrophic bacteria in sea water. Appl Environ Microbiol 41:518–527.

Torsvik V, Salte K, Srheim R, Goksyr J. 1990. Comparison of phenotypic diversity and DNA heterogeneity in a population of soil bacteria. Appl Environ Microbiol 56:776–781.

Tseng H-Y. 1997. A tectogenetic origin for the deep subsurface microorganisms of Taylorsville Basin, Virginia: thermal and fluid flow model constraints [PhD dissertation]. Princeton, NJ: Princeton University, 202 pp.

Tseng H-Y, Onstott TC, Burruss RC, Miller DS. 1995. Constraints on the thermal history of Taylorsville Basin, Virginia, U.S.A., from fluid-inclusion and fission-track analyses: implications for subsurface geomicrobiology experiments. Chem Geol 127:269–294.

Van Houten FB. 1965. Composition of Triassic Lockatong and associated formations of Newark Group, central New Jersey and adjacent Pennsylvania. Am J Sci 205:825–863.

Washburn FW. 1921. Note on a method of determining pore sizes in porous material. Proc Natl Acad Sci USA 7:115–116.

Weaver CE, Pollard LD. 1973. The chemistry of clay minerals. Amsterdam: Elsevier, 213 p.

Weems RE. 1980. The depositional history and structural development of the Triassic Taylorsville basin (east-central Virginia). In: Contributions to Virginia geology IV, Virginia Div Geol Pub 27, p 23–38.

White DC, Davis WM, Nickels JS, King JD, Bobbie RJ. 1979. Determination of the sedimentary microbial biomass by extractable lipid phosphate. Oecologia 40:51–62.

White DC, Pinkart HC, Ringelberg DB. 1996. Biomass measurements: biochemical approaches. In: CH Hurst, GR Knudsen, JJ McInerney, LD Stetzenbach, MV Walter, editors. Manual of environmental microbiology. Washington, DC: Am Soc Microbiol Press. p 91–101.

Zhang C, Liu S, Logan J, Mazumder R, Phelps TJ. 1996. Enhancement of Fe(III), Co(III), and Cr(VI) reduction at elevated temperatures and by thermophilic bacterium. Appl Biochem Biotechnol 57/58:923–932.

Zobell CE. 1947. Microbial transformation of molecular hydrogen in marine sediments, with particular reference to petroleum. Bull Am Assoc Petrol Geol 31:1709–1751.